Experimental aspects of jet Substructure in Atlas and CMS

Mario Campanelli
Deniz Sunar Cerci

Thanks to:
Tobias Fitschen
Andrea Malara
N. Norjoharuddeen
Neelam Kumari
Donato Troiano
Robert Les
Alex Sopio

cost
EUROPEAN COOPERATION IN SCIENCE & TECHNOLOGY
Funded by the European Union
COMETA

Outline

- “Standard” jet constituents and calibrations
- Machine Learning for jets
- Jet taggers
- Example measurements for/with substructure

Two different detectors for the same physics

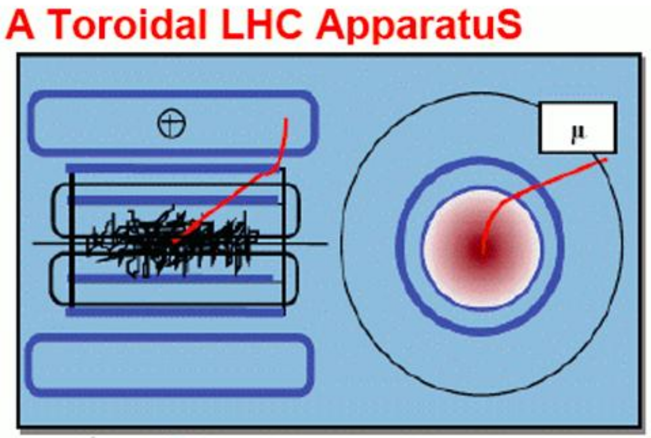

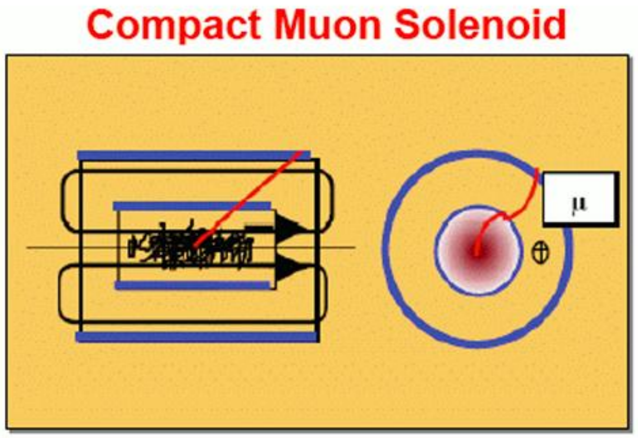

Tracking:

σ(pT), 1 GeV) = 1.3%
σ(pT), 100 GeV) = 3.8%

Tracking:

σ(pT), 1 GeV) = 0.7%
σ(pT), 100 GeV) = 1.4%

EM Calorimetry

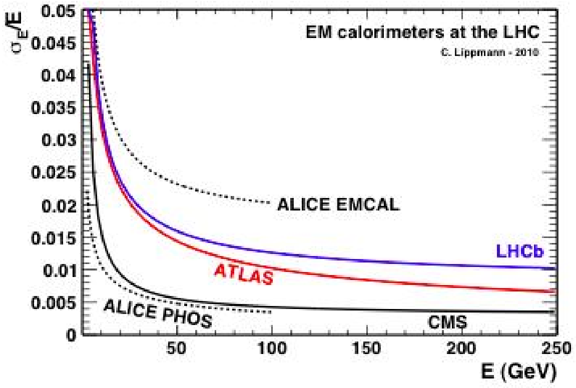

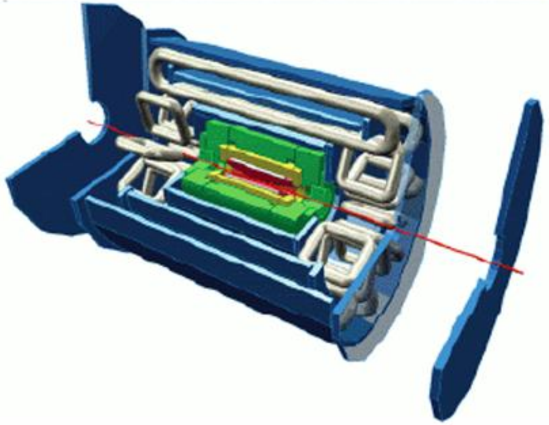

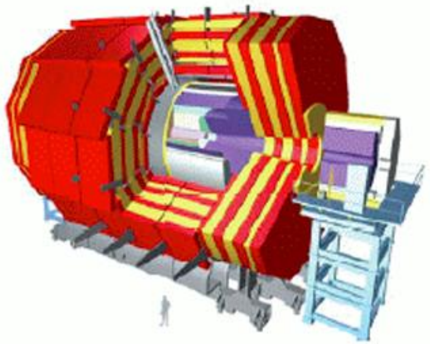

Had Calorimetry

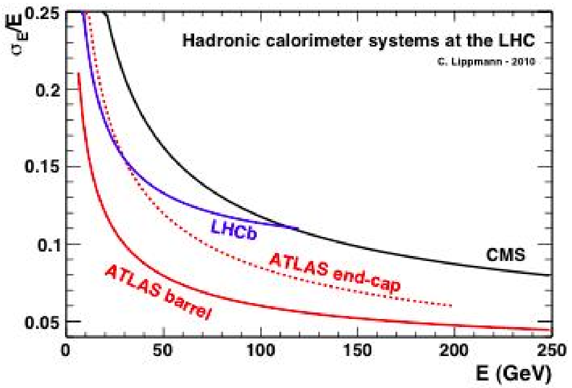

Jet reconstruction more based on calorimetry for ATLAS, more based on tracks (and PFlow) for CMS

From partons to detector: jet components

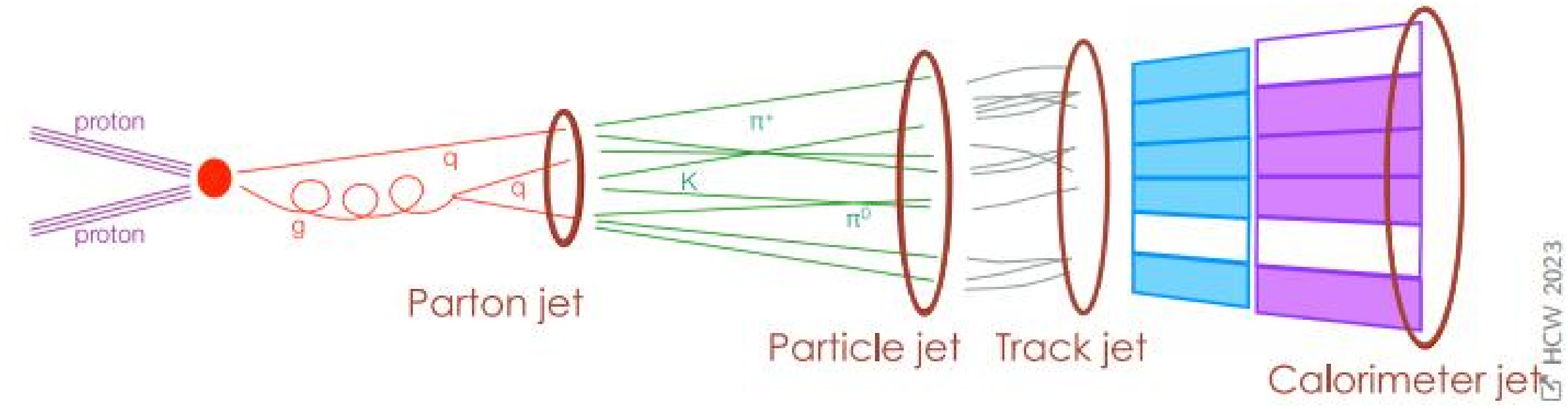

-Track jets easier to calibrate, and vertex can be used to mitigate pileup.
  but harder to compare to theory, and have bad pT resolution. Just used for substruture
- Calorimeter jets good at high-pt
  need to account for non-compensation,
  bad performanor the soft comcponent
  hard to control pileup
- Combined (PFlow) combine advantages of both
  hard to remove overlap and double counting

The basis of ATLAS jets: Topological Clusters

Eur. Phys. J. C 77 (2017) 490

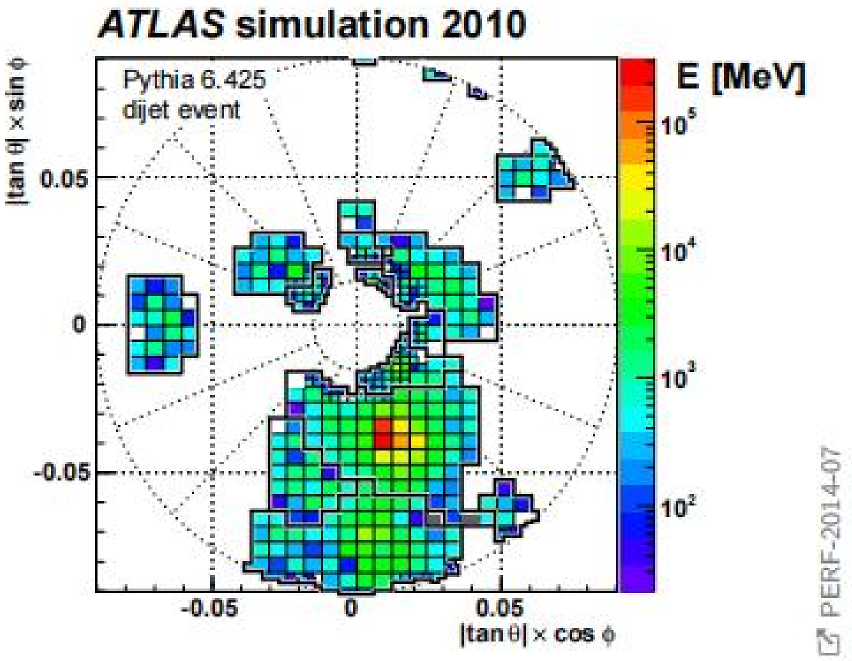

Cell noise ratio: $\zeta_{\text{cell}}^{\text{EM}} = \frac{E_{\text{cell}}^{\text{EM}}}{\sigma_{\text{noise,cell}}^{\text{EM}}}$

Topological Clusters

of E deposits in calorimeter cells

→ algorithm:

1 **Seed:** Find cells with energy $E > 4 \times |\zeta|$

2 **Growth:** Neighbors with $E > 2 \times |\zeta|$ are added

3 **Boundary:** any neighboring cells are added

(no ζ requirement)

4 **Split:** Breaks up clusters with multiple maxima

Jets build from TopoClusters are called **EMTopo** Jets

EM: Electromagnetic scale

→ ATLAS calorimeters are non-compensating

→ EM response ≈ 1, hadronic response < 1

Local Cluster Weights for ATLAS TopoClusters

Eur. Phys. J. C 77 (2017) 490

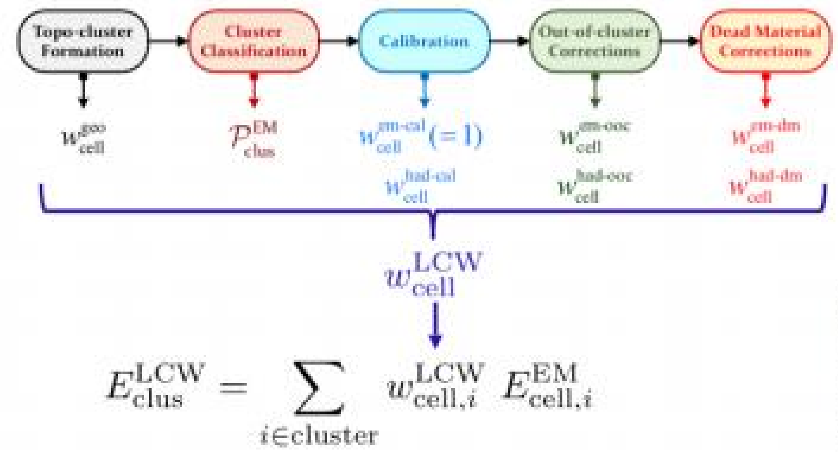

HCW 2023

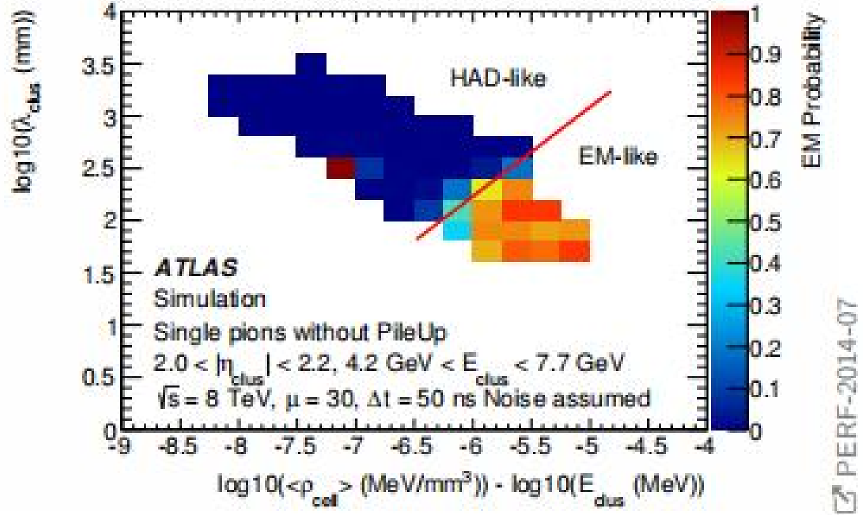

PERF-2014-07

- TopoClusters are identified to be EM or had by likelihood $\mathcal{P}^{\mathrm{EM}}_{\mathrm{clus}}$
- Their momenta are reweighted (ω) by
  - Difference in response due to non-compensating calorimeter
  - Energy falling in unclustered cells
  - Inactive/dead regions of the detector

Jets build from TopoClusters+LCW are called **LCTopo** Jets
used for large-R ($R = 1.0$) jets in Run 2

Particle flow and Track-Calo Clusters in ATLAS

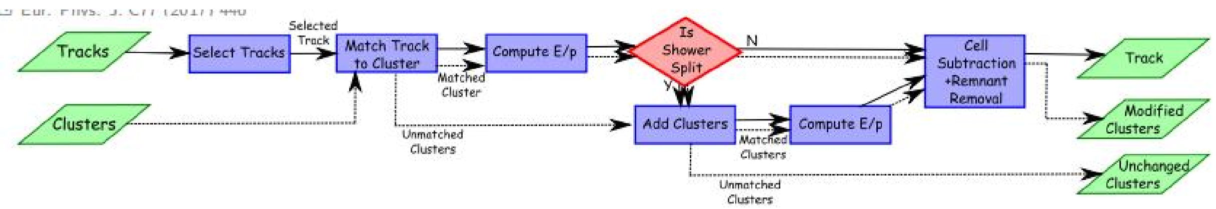

PFlow makes use of tracking information at constituent level

shows great JER improvement over calo jets in low-pT

Especially in the central region

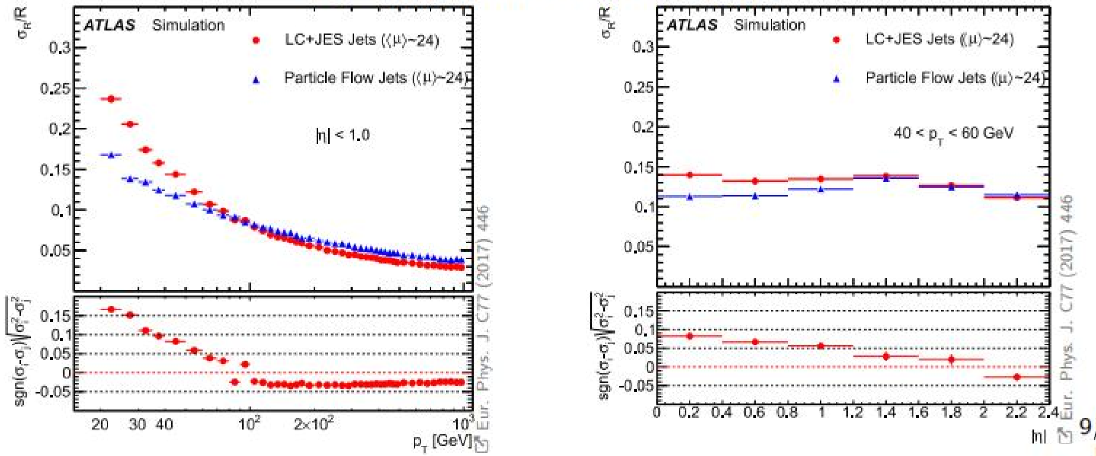

9/21

P-flow objects start from TopoClusters and assiciate tracks. Improves jet energy resolution

- Resolution-based track-to-cluster matching

$$\Delta R < \sqrt{\sigma^2_{\text{cluster}} + \sigma^2_{\text{track}}}$$

- resulting in 3 different constituents:
  - **combined:** clusters matched to tracks from primary vertex (PV)
  - **charged:** tracks from PV not matched to any cluster
  - **neutral:** clusters not matched to any track (from the PV)
  - Clusters matched to tracks from PU vertices are **discarded**

TCC start from tracks and consider their associations to clusters. Designed for substructure studies

The synthesis: Unified Flow Objects (UFO)

Eur. Phys. J. C 81, 334 (2021)

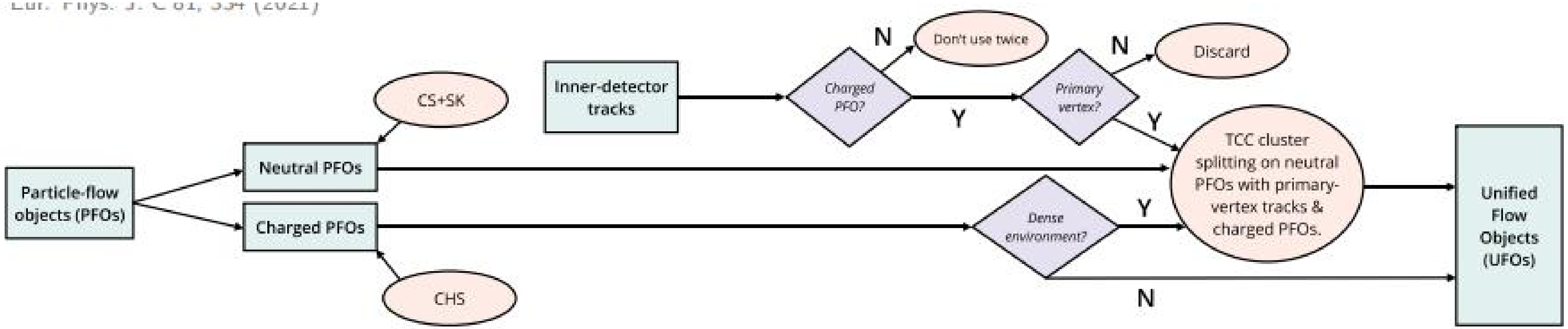

PFlow Shows best jet mass and p_T resolution at low p_T

TCC performs better at high p_T

UFO combines the best of both

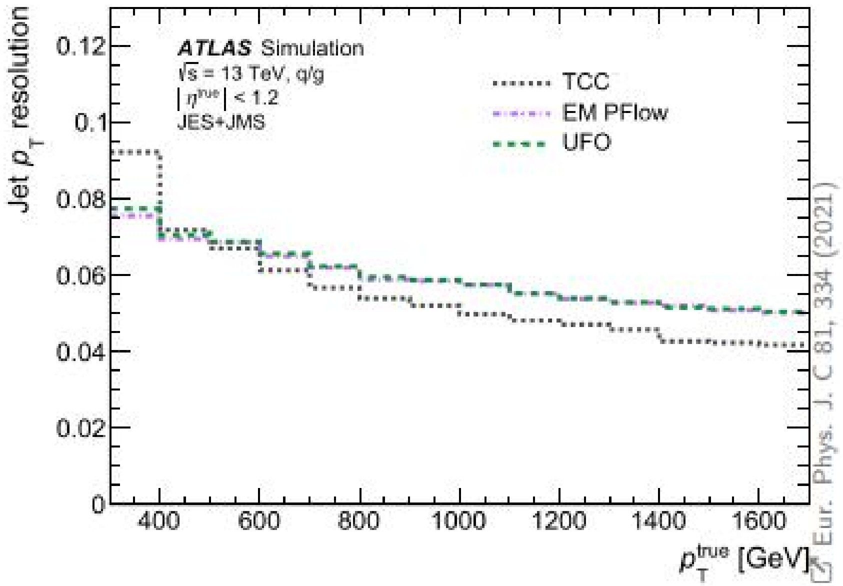

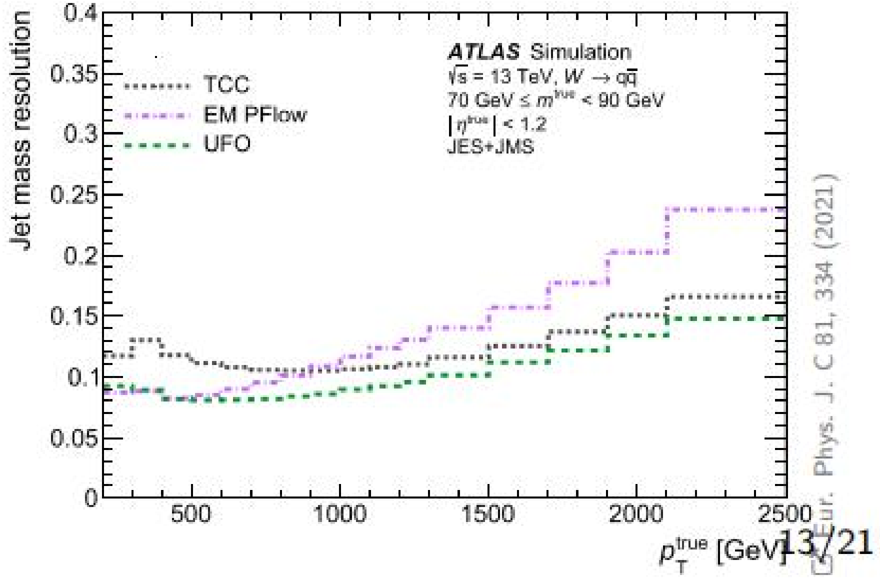

Jet inputs in CMS

Local reconstruction: Tracks, ECAL, HCAL →	▶ Information from sub-detectors ▶ Similar method online but less detail
Particle flow (PF) →	▶ Link tracks and calorimeter signals ▶ Particle identification

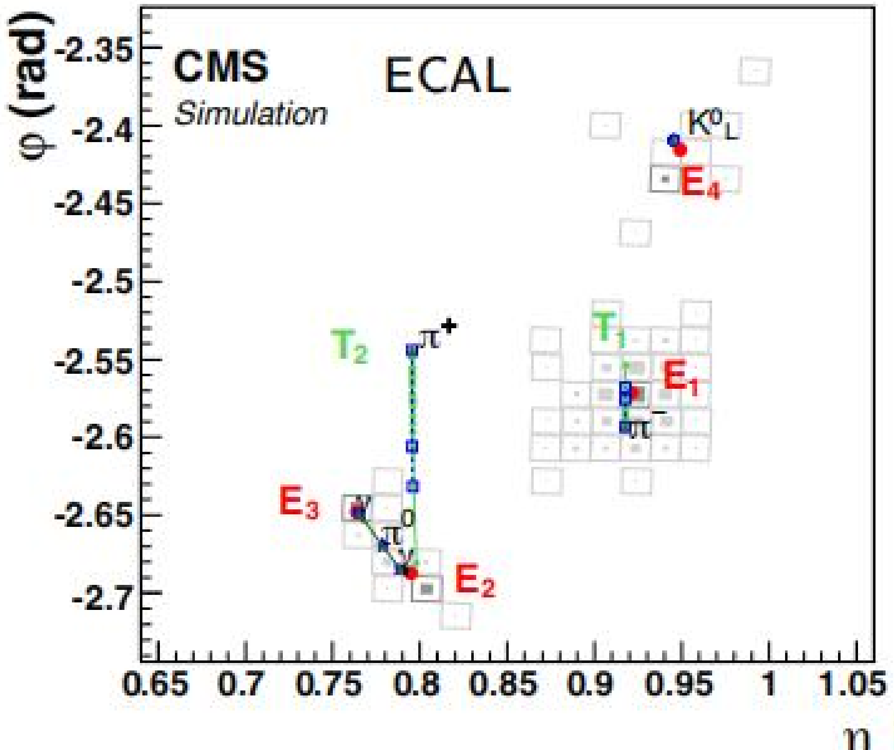

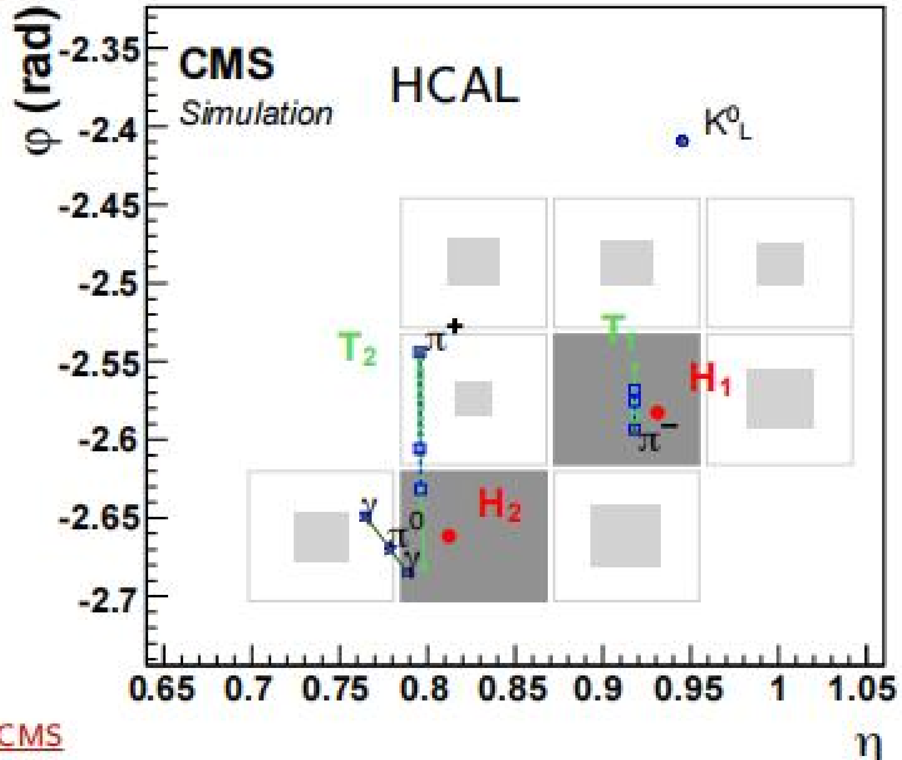

Particle Flow in CMS

Jet calibration in CMS

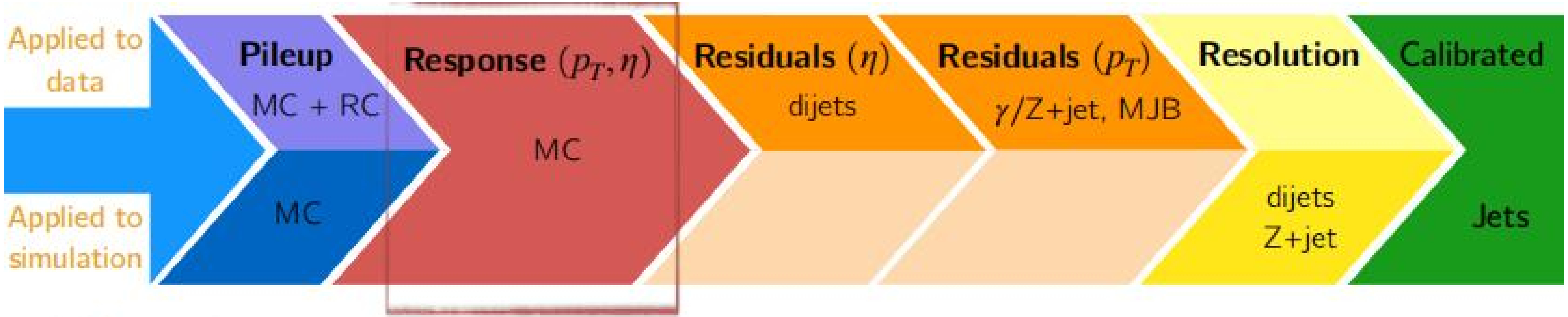

MC truth correction:

PU subtraction

Jet response calibration

- Core of the calibration
- Simulation-based
- Accounts for detector effects
- Change in performance due to detector acceptance
- Closure better that 1% everywhere (0.1% in central region)

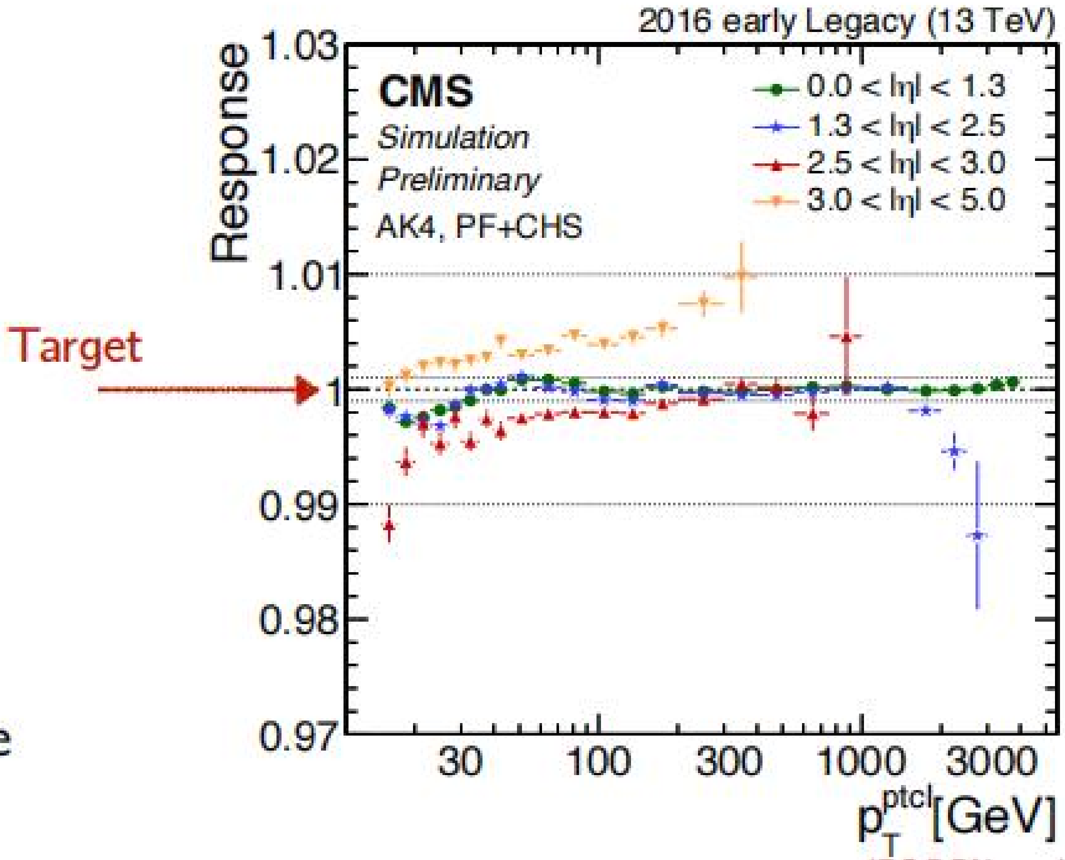

Residual corrections for CMS calibration

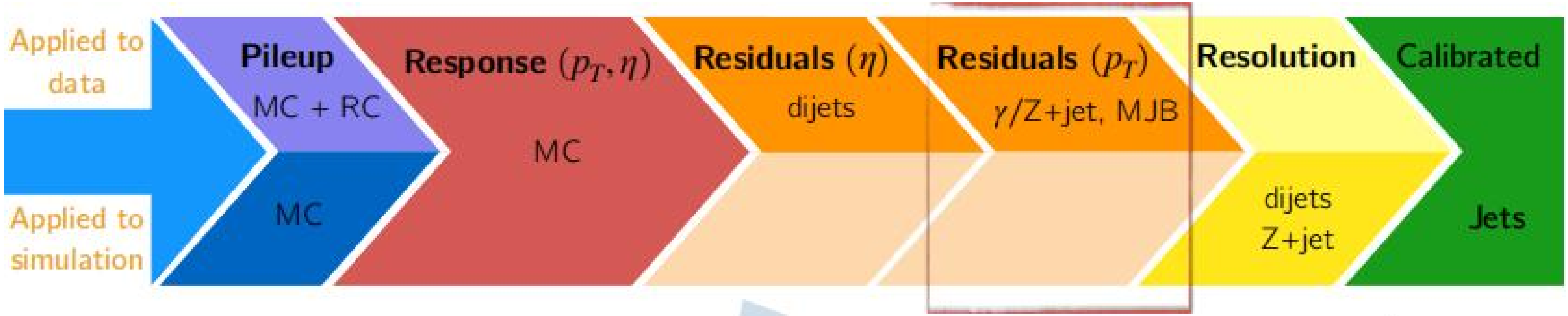

MC truth correction:

PU subtraction

Jet response calibration

Residual corrections

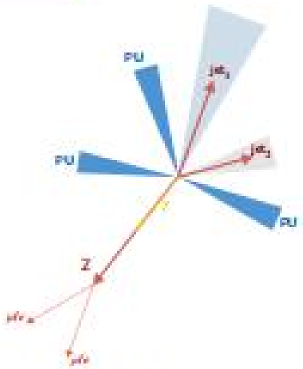

- Additional p_{T} -dependent corrections accounting for absolute scale in barrel
- Determined relative to precisely measured reference objects (μ, e, γ, W)
- Channels combined in a global fit
  - Exploit individual precision in each phase-space

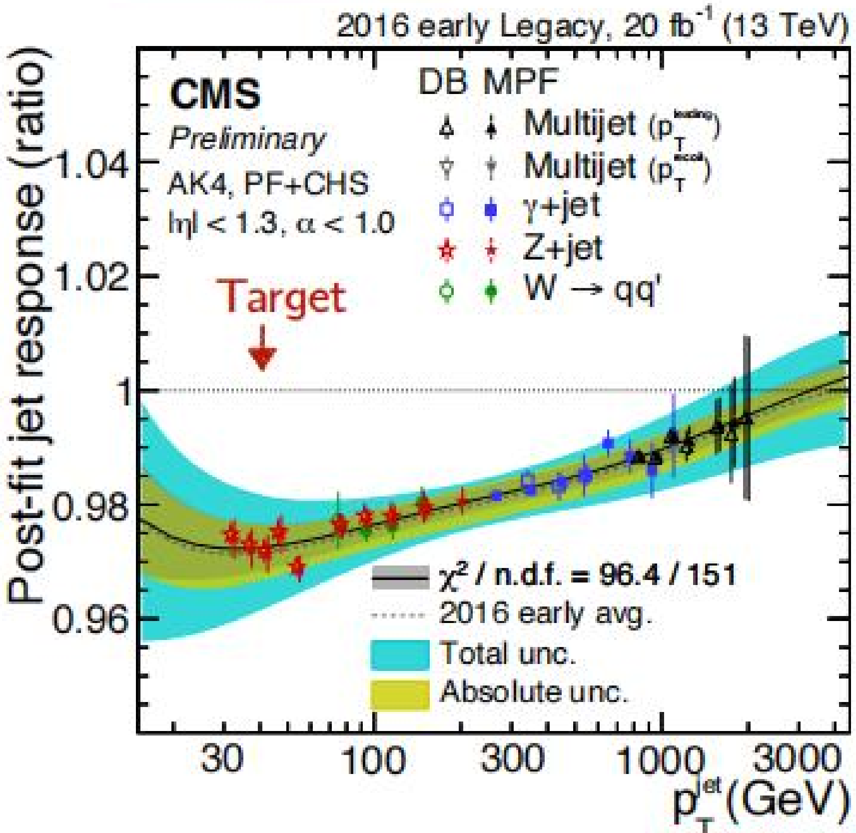

JEC DPNotes Legacy

CMS: jet energy scale uncertainty

MC truth correction:

- PU subtraction
- Jet response calibration

Residual corrections

Jet energy resolution smearing

Jet energy scale uncertainties

- Uncertainty ~1% for jets pt >100 GeV
- Increasing contribution from PU
- Detector degradation:
  - Ageing, damage, ...

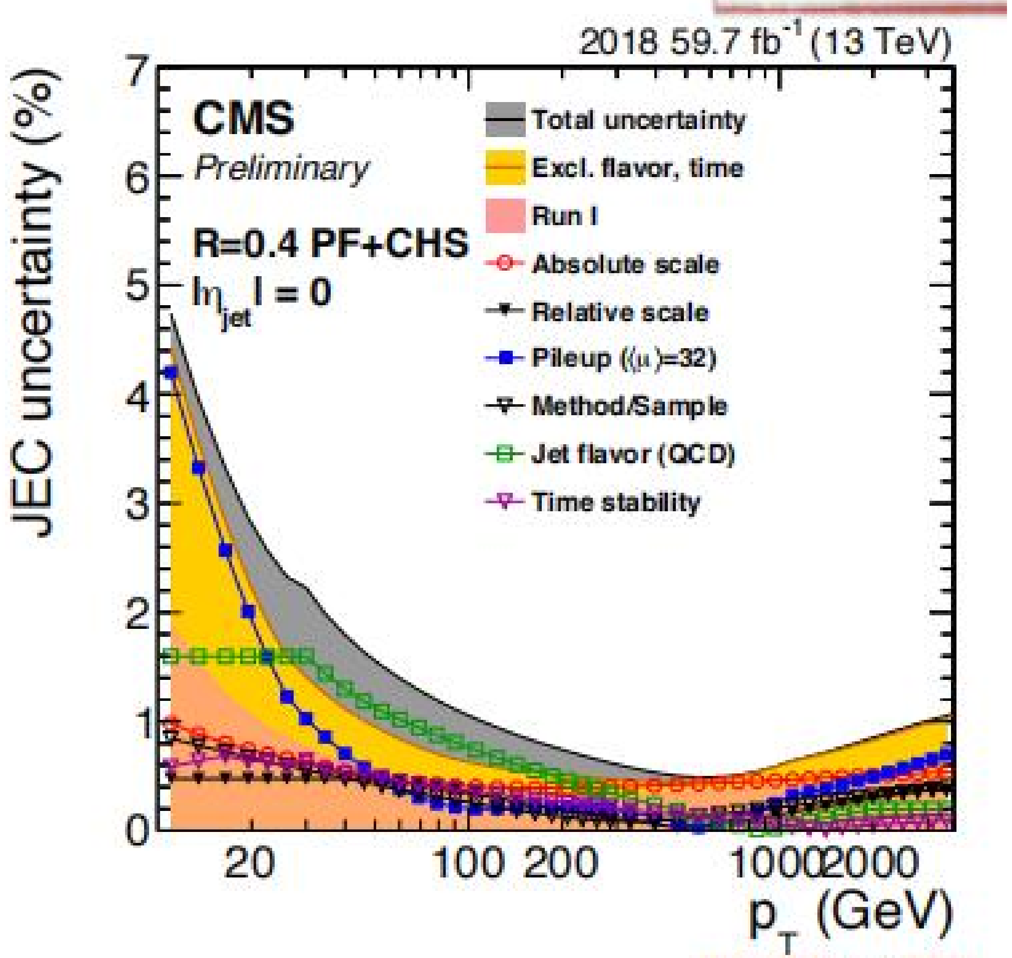

JEC DPNotes EOY

Calibrating jets in ATLAS

Eur. Phys. J. C 81 (2021) 689

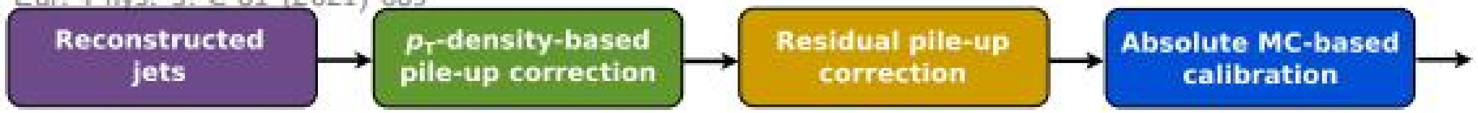

- Calculate E response in bins of η and E_{true} in MC
- Numerical inversion yields calibration factors
- Origin correction corrects jet η
- Largest calibration step that brings response on average to 1

$$R(E_{\text{jet}}^{\text{truth}}, \eta_{\text{det}}) = E_{\text{jet}}^{\text{reco}} / E_{\text{jet}}^{\text{truth}}$$

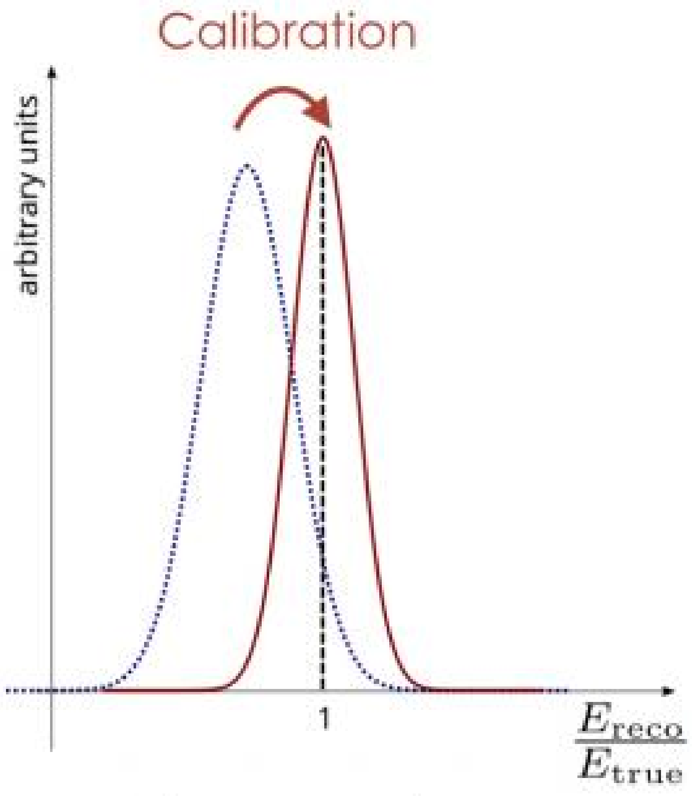

$$R(E_{\text{jet}}^{\text{truth}}, \eta_{\text{det}}) \rightarrow R^{-1}(E_{\text{jet}}^{\text{reco}}, \eta_{\text{det}})$$

HCW 2023

Global Sequential Calibration and In-Situ corrections

p_T **response** after each GSC step

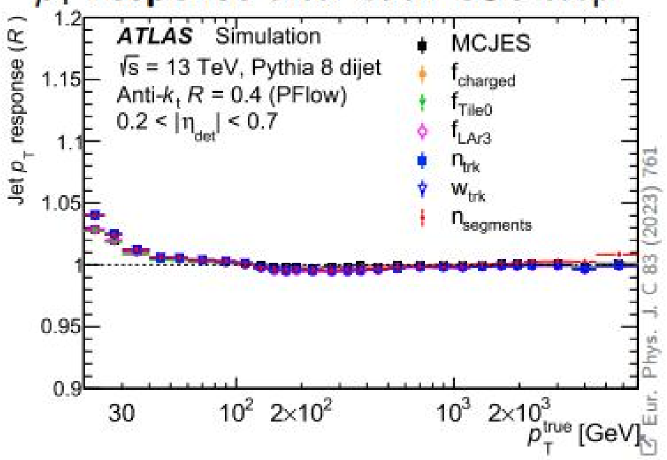

Global Sequential Calibration

- After energy scale calibrated on average, **GSC** corrects for small differences
- E.g. for different jet flavours
- **Sequentially** corrects for each variable
- Only for small (R=0.4) jets

GSC improves JER by applying different cor
for different population of jets (e.g. q/g in
but leaves JES on average the same

In-situ calibration in data
Corrects jets with high uncertainty (e.g. forward)
based on well-known (photons, central jets...) objects

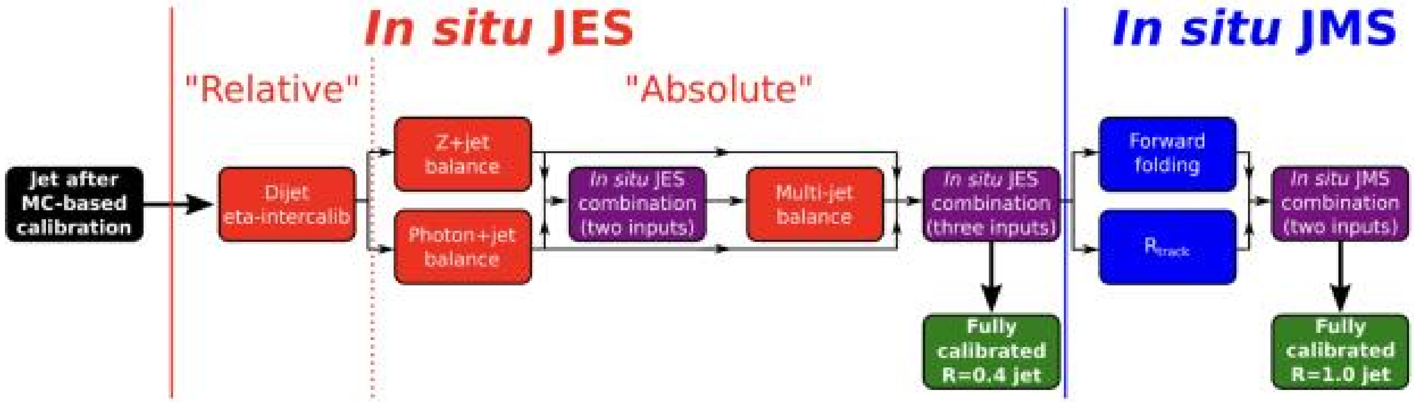

ATLAS JES resolution and uncertainty

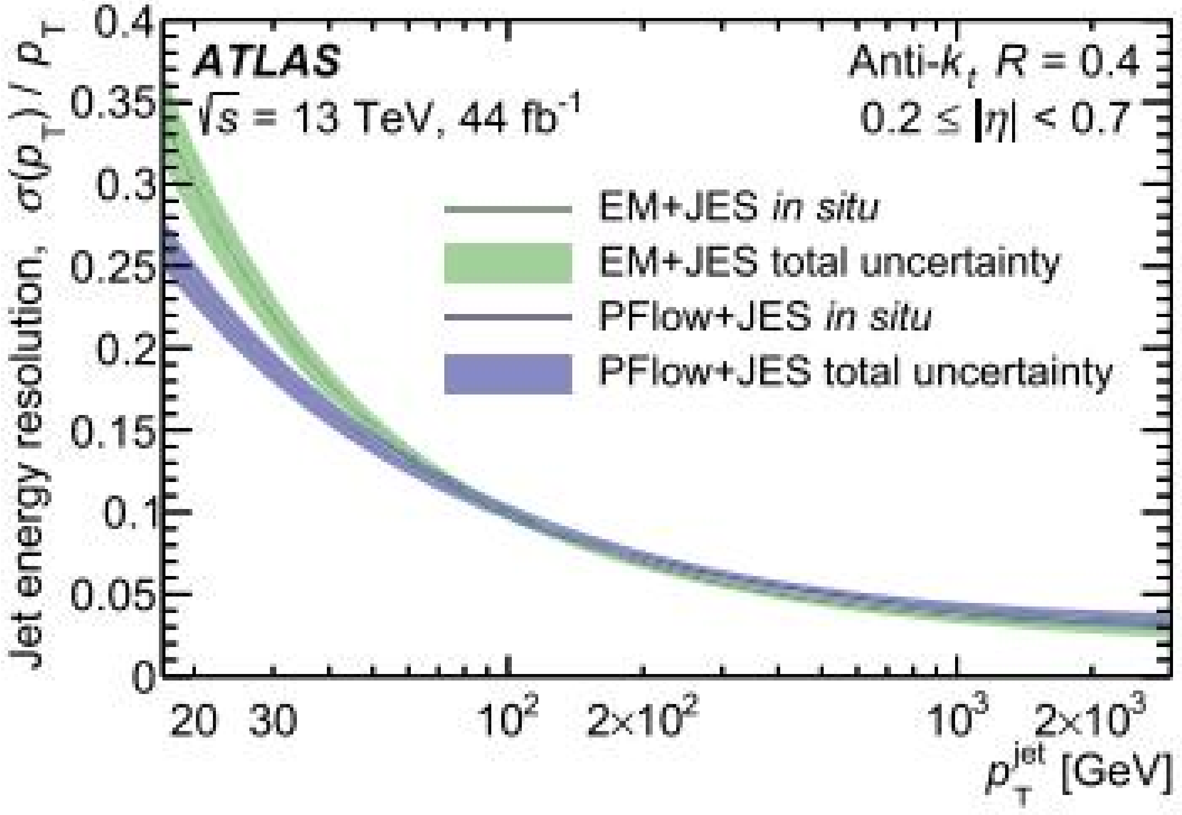

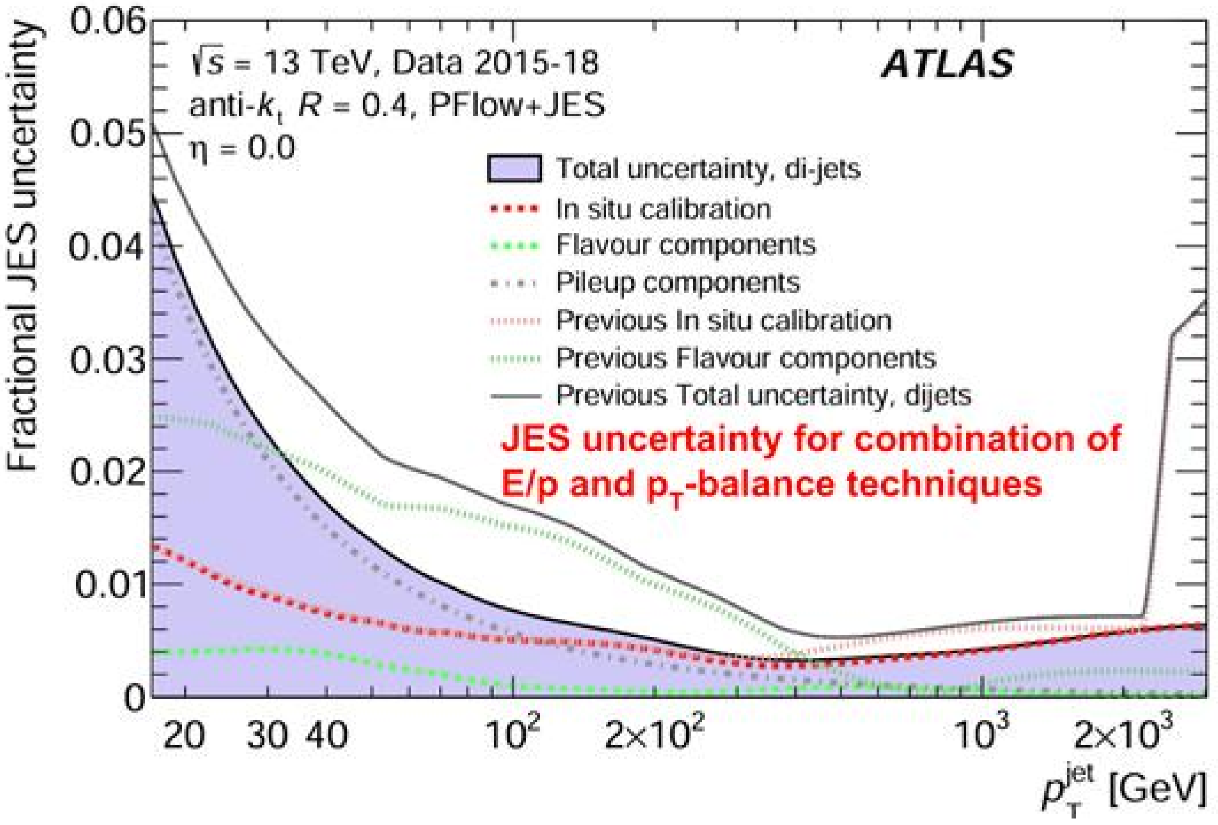

Also 1% uncertainty after in-situ corrections

Pileup mitigation in CMS

Charged Hadron Subtraction (CHS)

- Tracker information to remove charged particles associated to PU
- Neutral particles energy subtracted
- Applicable for $|\eta| < 2.4$

Pileup Per Particle Identification (Puppi) Puppi in CMS

- Per-particle weight
- Scale 4-momentum before clustering
- Charged particles similar to CHS
  - Redefined track-vertex association

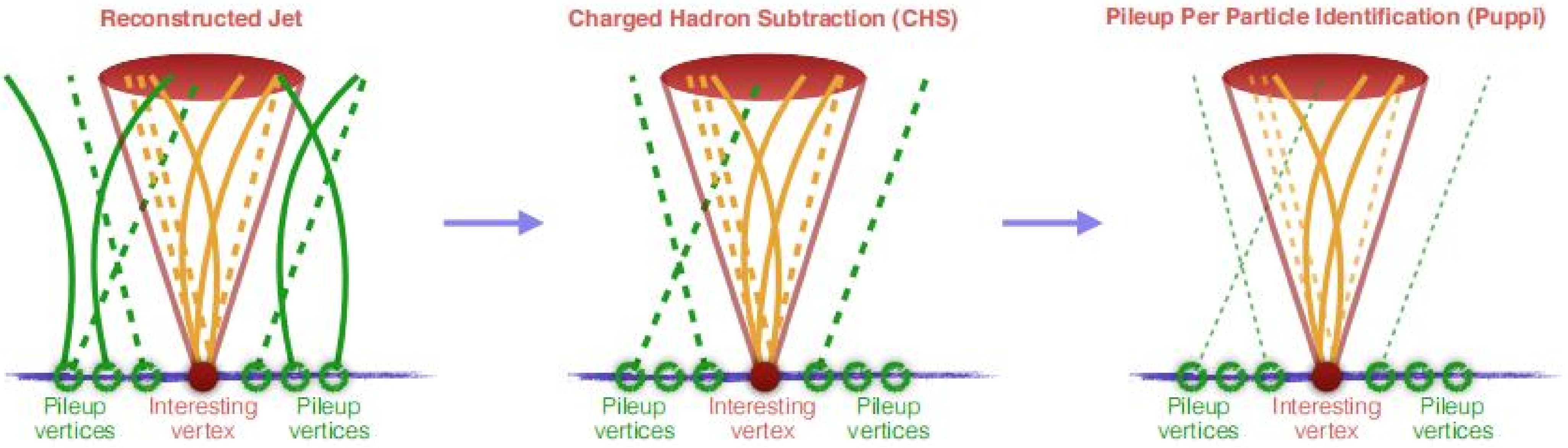

Performance of PUPPI in CMS

- Widely used in Run 2, default in Run 3
- Improved all jet-related variables
  - Jet efficiency and purity (matched to generator-level jets)
  - Jet substructure
  - New optimation to include hadronic tau reconstruction: CMS-DP-2024-043

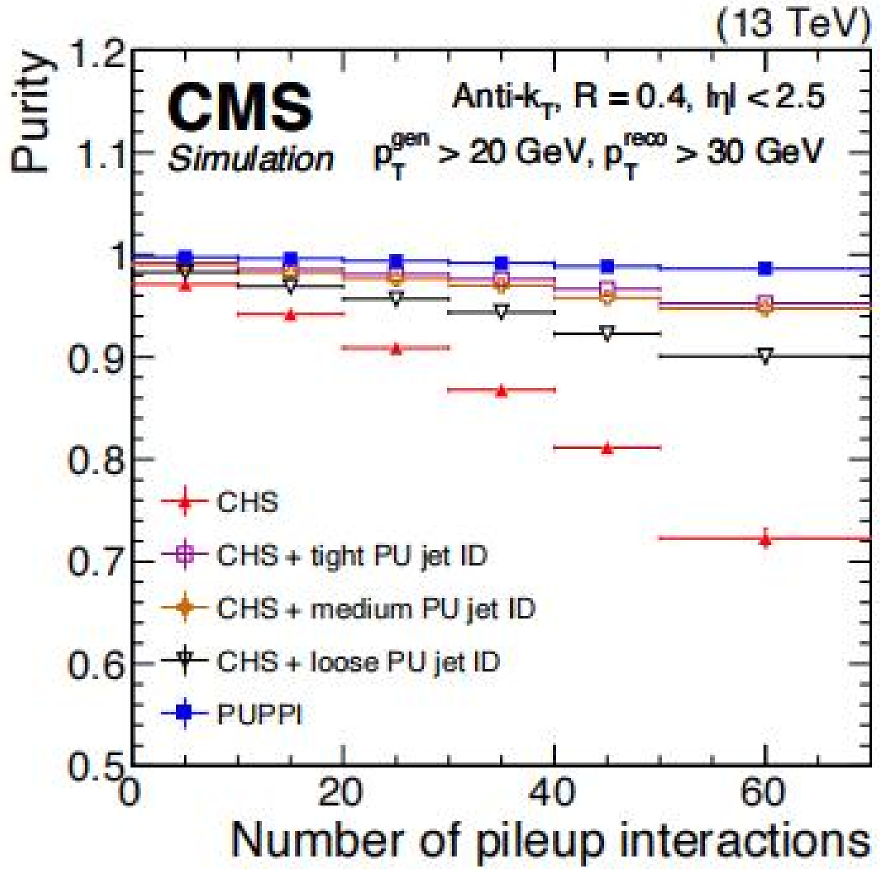

CMS-DP-2021-001

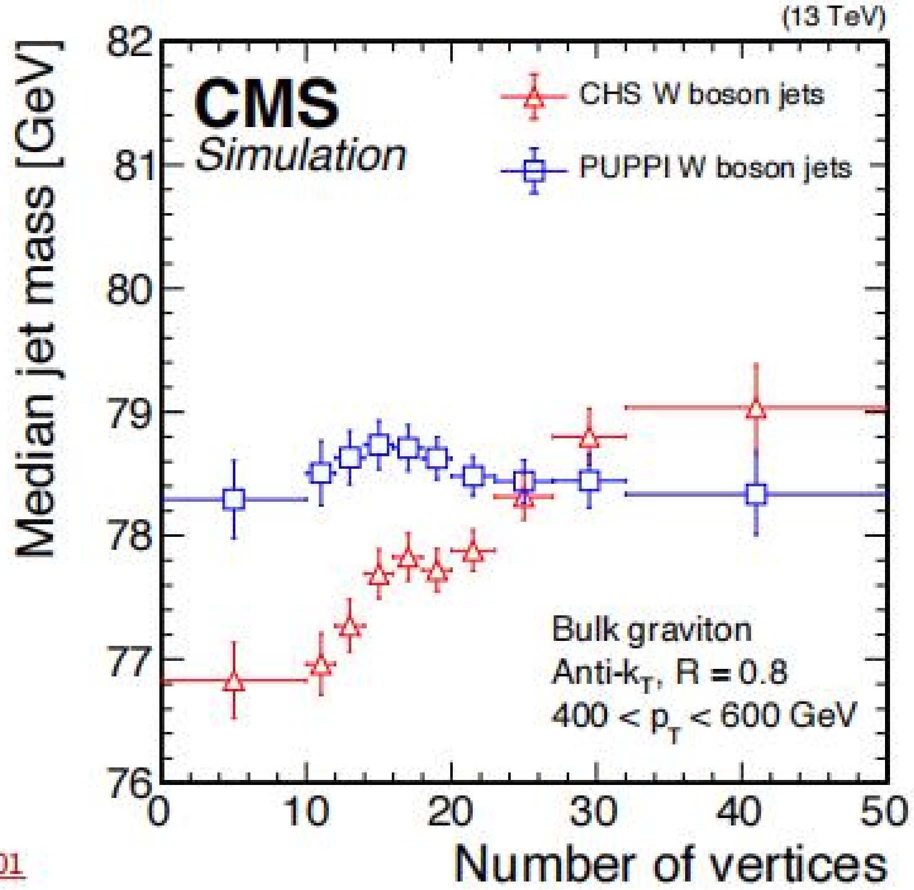

Pileup mitigation in ATLAS: constituent subtraction and SoftKiller

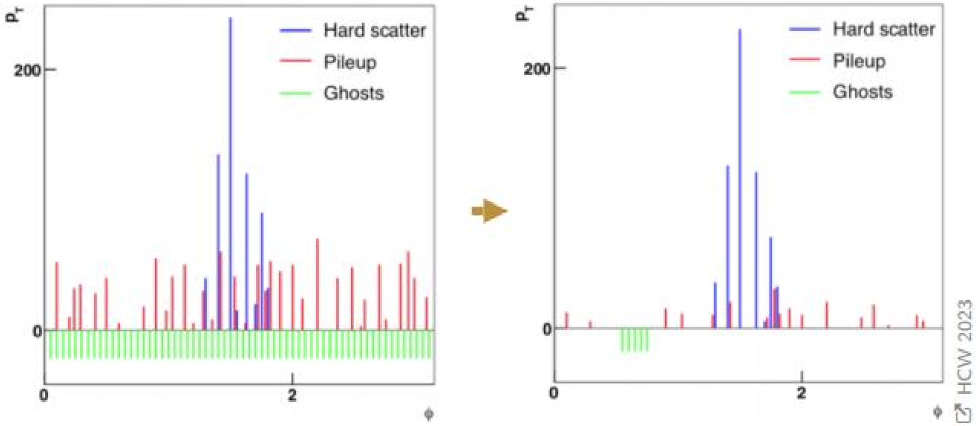

- Add ghosts in grid of $A_g = \eta \times \phi = 0.1 \times 0.1$
- With $p_T^g = A_g \times \rho$
  - $\rho = \text{med}\{\frac{p_T}{A}\}$: median energy density in event
  - Measure of PU in event
- Subtract p_T^g from p_T of constituents c within $\Delta R(g, c)$

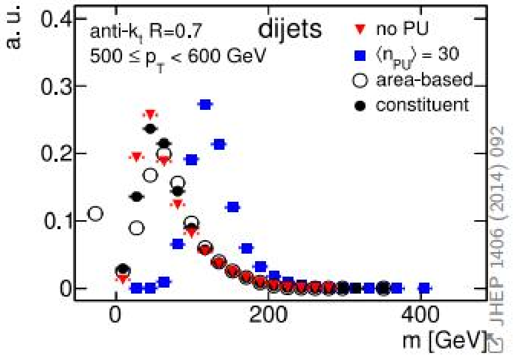

Mass profile with CS closer to no-PU than with area-based alone 6/21

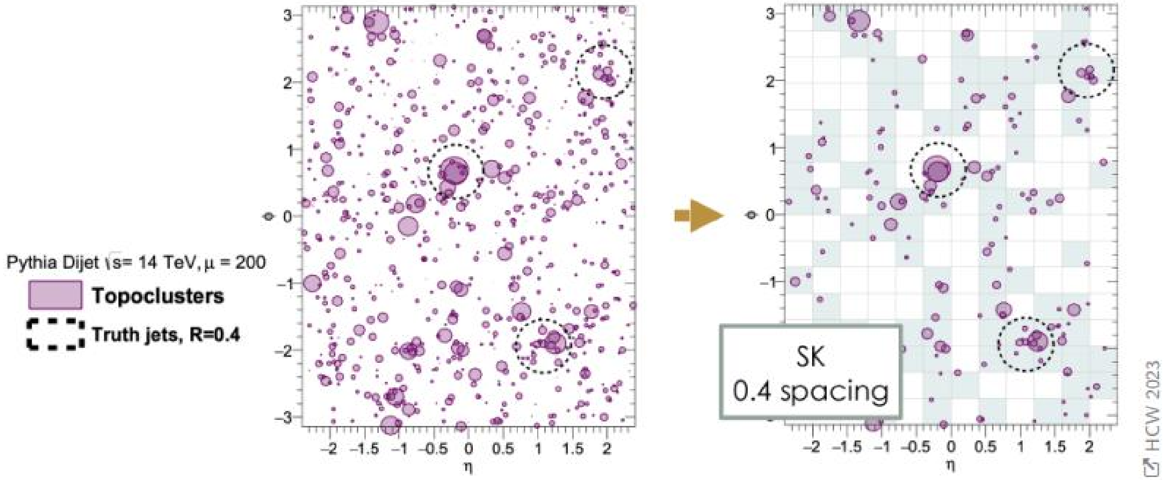

- CS: Scales constituents
- SK: Removes constituents
- Consider constituents in η, ϕ grid
- All constituents with $p_T < p_T^{\text{cut}}$ are removed
- p_T^{cut} determined such that half of grid cells are empty

ATLAS uses CS+SK for R=1.0 jets

Improving TopoClusters calibration with Machine learning (ATLAS)

First step in cluster calibration: Differentiate EM from hadronic clusters

Non-compensating ATLAS calorimeter requires different calibrations for neutral/charged clusters

π^0 vs $\pi^\pm$ classification performance

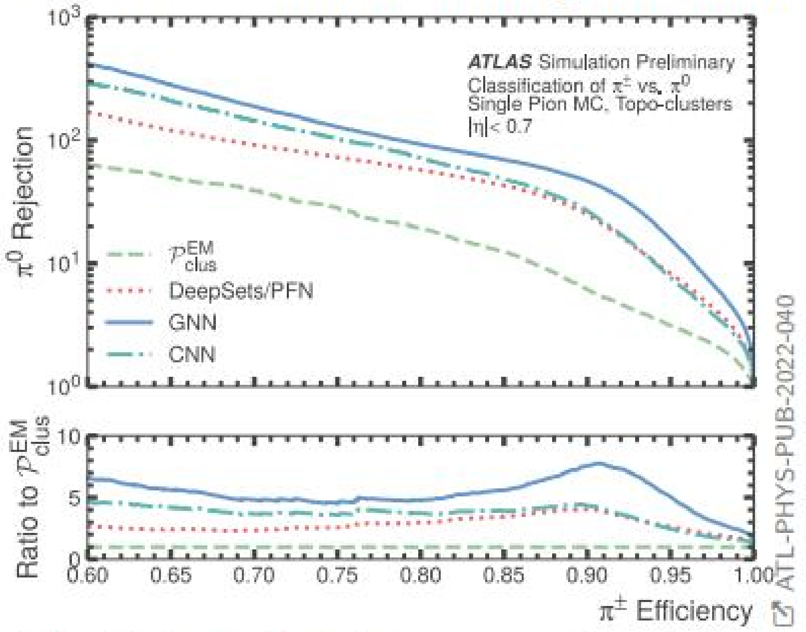

Point cloud of energy deposits in calorimeter cells

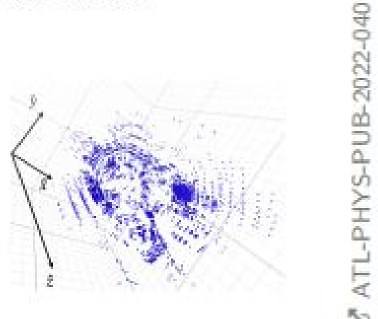

Image: $\pi^0 - \pi^\pm$ difference

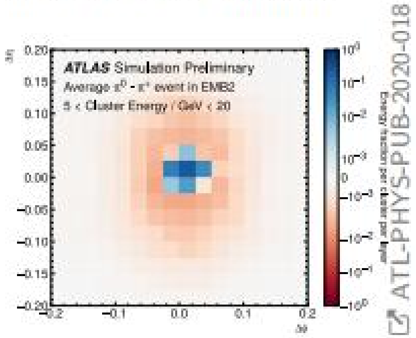

Baseline used in LCW: $\mathcal{P}^{EM}_{clus}$

- Binned EM-scale cluster variables
  - Total cluster energy $E^{EM}_{cluster}$
  - Pseudorapidity η
  - Longitudinal depth λ_{clus}
  - 1st cell energy moment $\langle\rho_{cell}\rangle$
- Combined into likelihood $\mathcal{P}^{EM}_{clus}$

Individual calorimeter cell signals

→ As point clouds (**GNN**, **PFN**)

→ Or projected on images (**CNN**)

Observations

- All point cloud methods significantly outperform baseline $\mathcal{P}^{EM}_{clus}$

Topo Cluster energy calibration with ML

First step in cluster calibration: Differentiate EM from hadronic clusters
Non-compensating ATLAS calorimeter requires different calibrations for neutral/charged clusters

π^0 vs $\pi^{\pm}$ classification performance

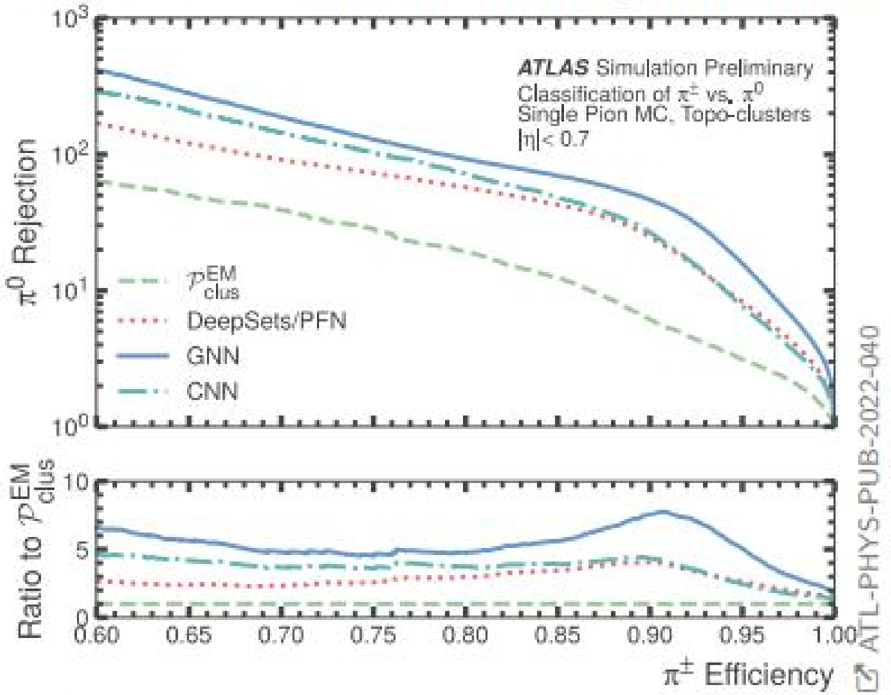

Point cloud of energy deposits in calorimeter cells

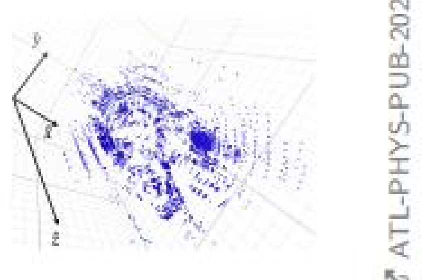

Image: $\pi^0 - \pi^{\pm}$ difference

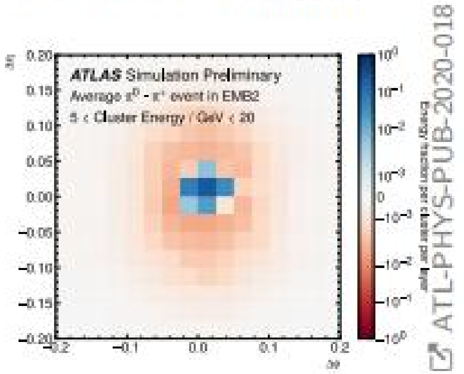

Baseline used in LCW: $\mathcal{P}^{EM}_{clus}$

- Binned EM-scale cluster variables
  - Total cluster energy $E^{EM}_{cluster}$
  - Pseudorapidity η
  - Longitudinal depth λ_{clus}
  - 1st cell energy moment $\langle\rho_{cell}\rangle$
- Combined into likelihood $\mathcal{P}^{EM}_{clus}$

Individual calorimeter cell signals

→ As point clouds (**GNN**, **PFN**)

→ Or projected on images (**CNN**)

Observations

- All point cloud methods significantly outperform baseline $\mathcal{P}^{EM}_{clus}$

4/21

Global Neural Network jet Calibration

Response

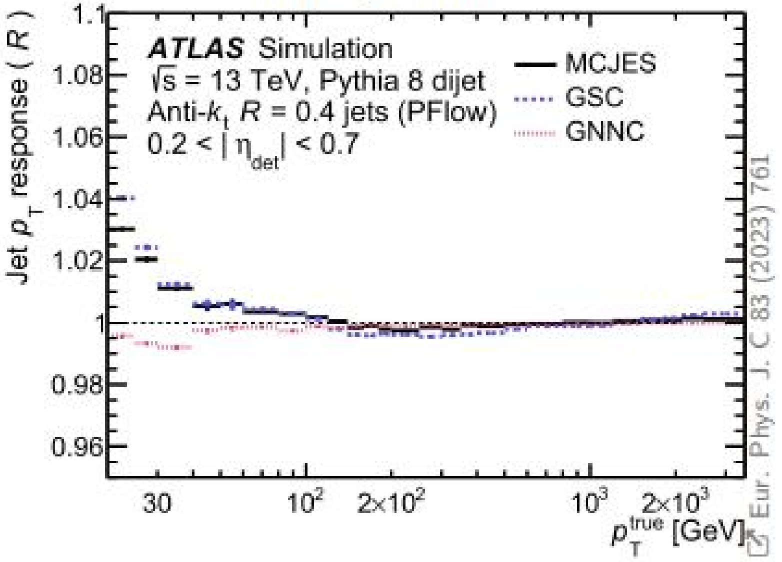

Global NN Calibration (GNNC)

- **GSC** Does not exploit correlations of variables
- New method (**GNNC**) uses MLP trained to predict p_T response

→ Improvement over full p_T range

Resolution

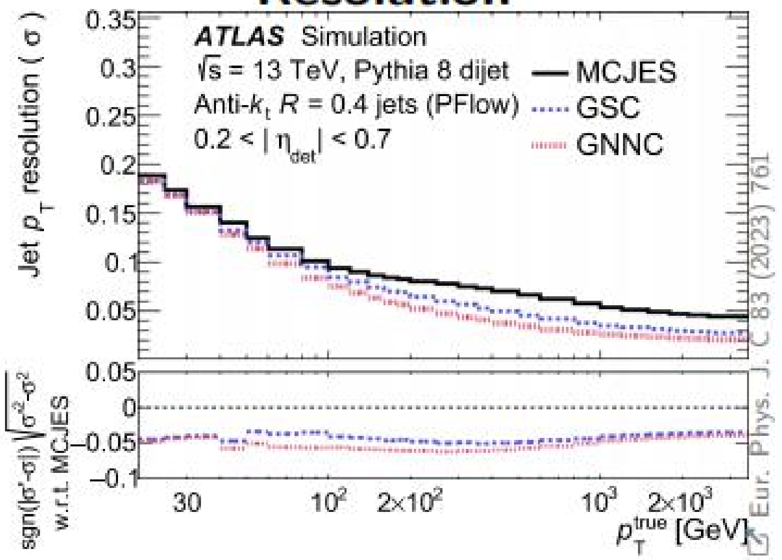

Flavour Uncertainty

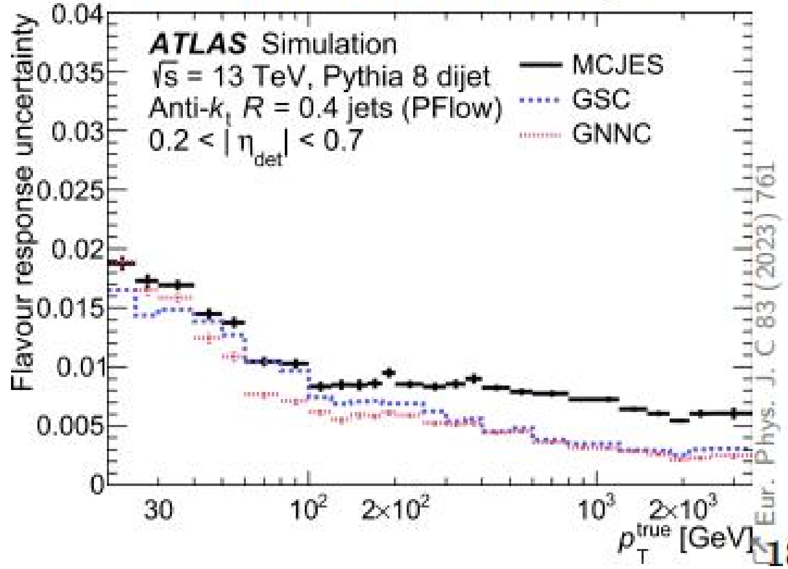

Simultaneous calibration of energy and mass

Model Architecture

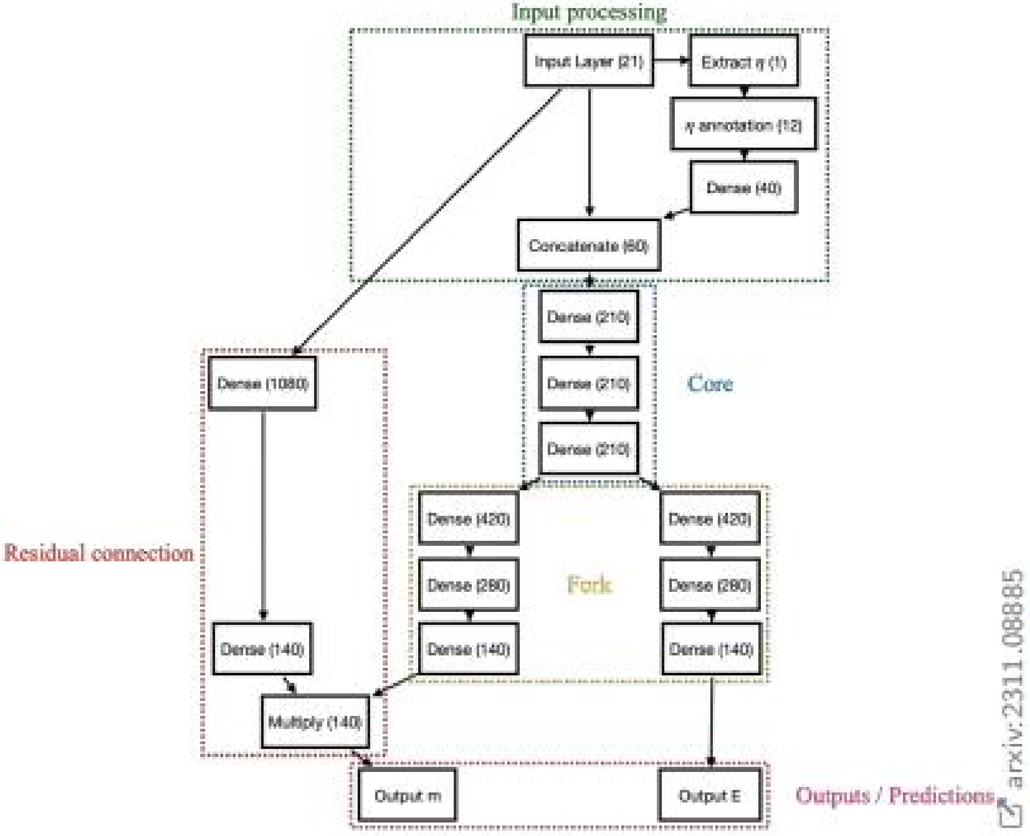

Method:

- Predict responses

$$R_E = \frac{E_{\text{reco}}}{E_{\text{true}}},\ R_M = \frac{M_{\text{reco}}}{M_{\text{true}}}$$

- Modeled by Gaussians

$$y_{\text{pred}} = (\mu^E, \sigma^E, \mu^m, \sigma^m)_{\text{pred}}$$

$\Rightarrow$ Calibration Factors:

$$E_{\text{calib}} = \frac{E_{\text{reco}}}{\mu^E_{\text{pred}}},\ M_{\text{calib}} = \frac{M_{\text{reco}}}{\mu^M_{\text{pred}}}$$

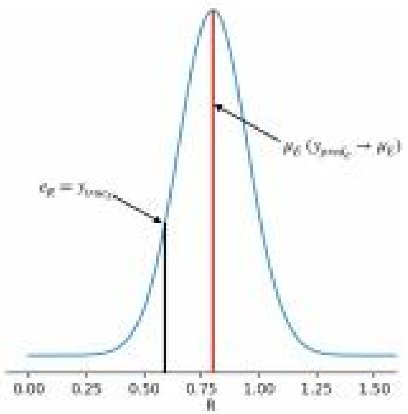

Mixture density network (MDN) loss:

$$\mathcal{L}_{\text{MDN}} = -\log(P(y_{\text{true}}, y_{\text{pred}})) = \log(\sigma_{\text{pred}}) + \frac{1}{2}\frac{(y_{\text{true}} - \mu_{\text{pred}})^2}{\sigma^2_{\text{pred}}}$$

Results for NN calibration

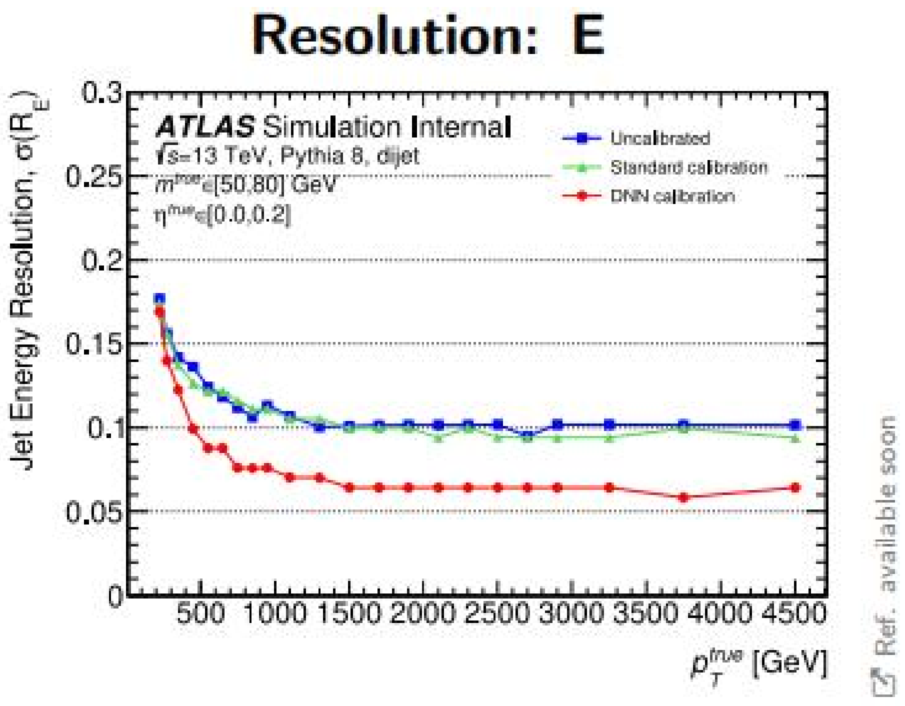

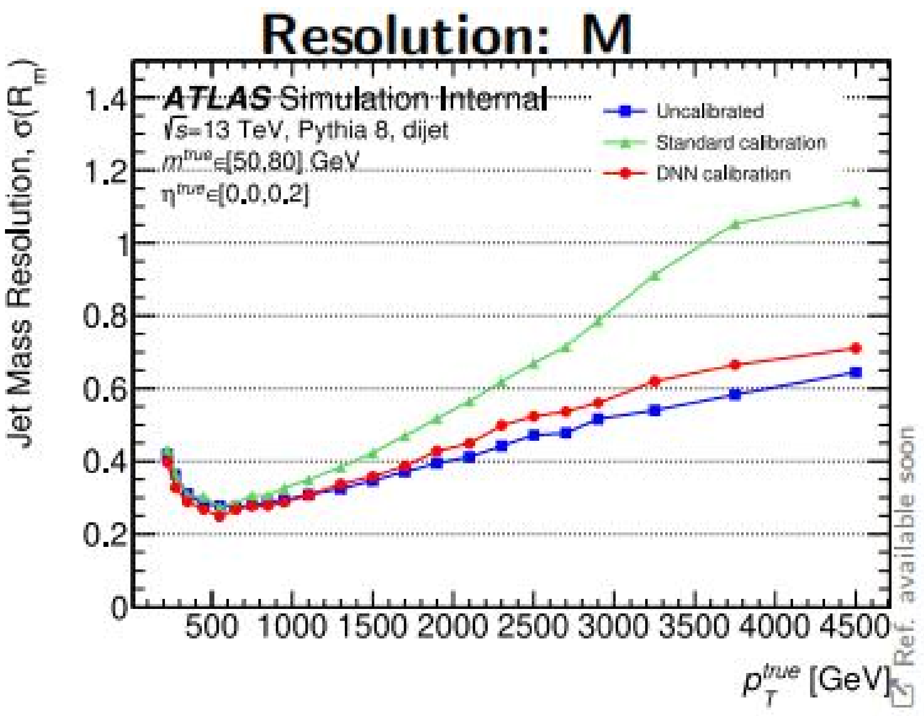

Improvement across the board

- **DNN**: better closure than **standard** calib. in response for E and M
- M response stable even in low and high p_T regime
- Resolution drastically improved
- Less dependence on η, pileup, MC generator for E and M
- More stable across different processes (H, W/Z, top) for E and M
- More stable across different flavours (q/g) for E and M

Pt calibration with ParticleNet (CMS)

Phys. Rev. D 101, 056019 (2020)

Graph NN with PF constituents & Secondary Vertices as inputs.

- First used for boosted resonance **tagging** with **AK8 jets**. DP-2020-002 CMS-PAS-BTV-22-001
- Extended for **AK8** jet **mass regression**. DP-2021-017
- Commissioned for **AK4** jet flavor tagging & p_T regression.

DP-2024-066

Classification	Regression	Quantile regression (resolution estimation)

$$L = CatEntropy(x, x_{truth}) + \gamma_{regr} \cdot log(cosh(y - y_{truth})) + \gamma_{quantile} \cdot [p_{0.16}(z - z_{truth}) + p_{0.84}(z - z_{truth})]$$

Two types of target p_T regression

without & with neutrino contribution

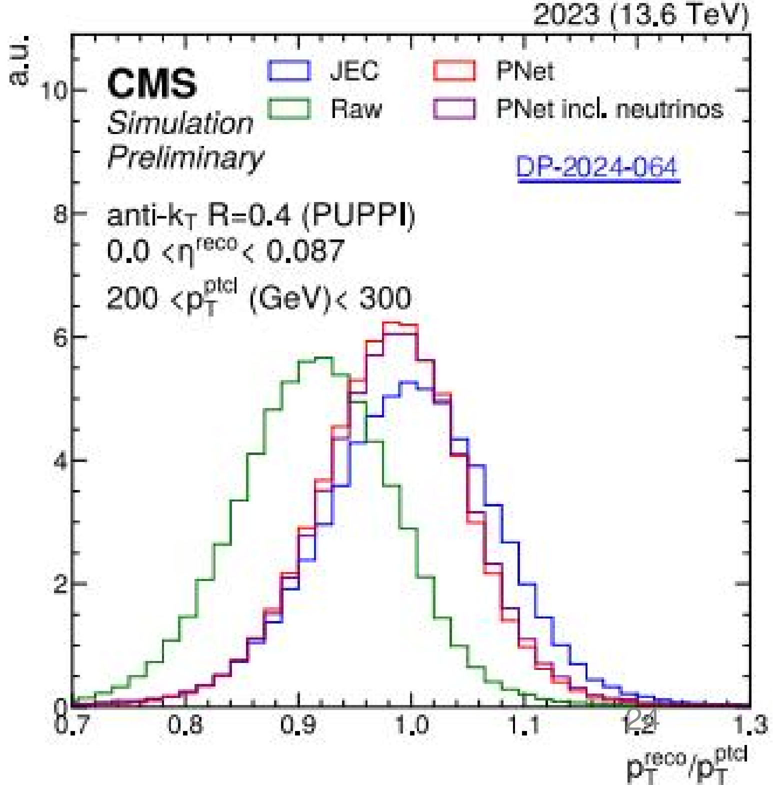

ParticleNet response

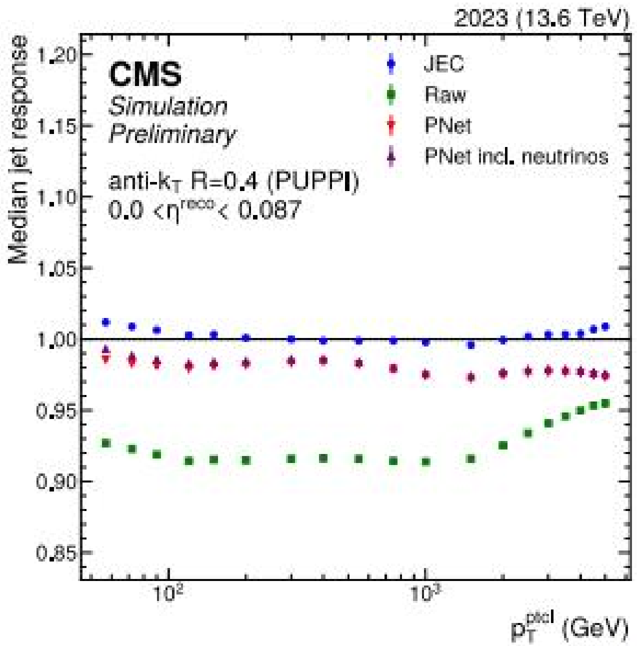

DP-2024-064

- Regressed p_T response closer to 1 compared to raw p_T for central jets.
- Derive MC-truth corrections, achieve response closure within 1% (similar level to JEC).

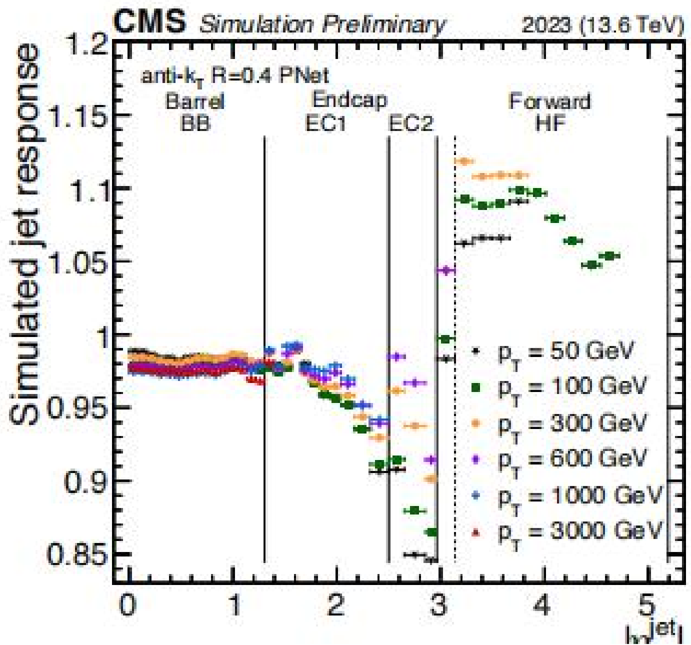

Apply corrections

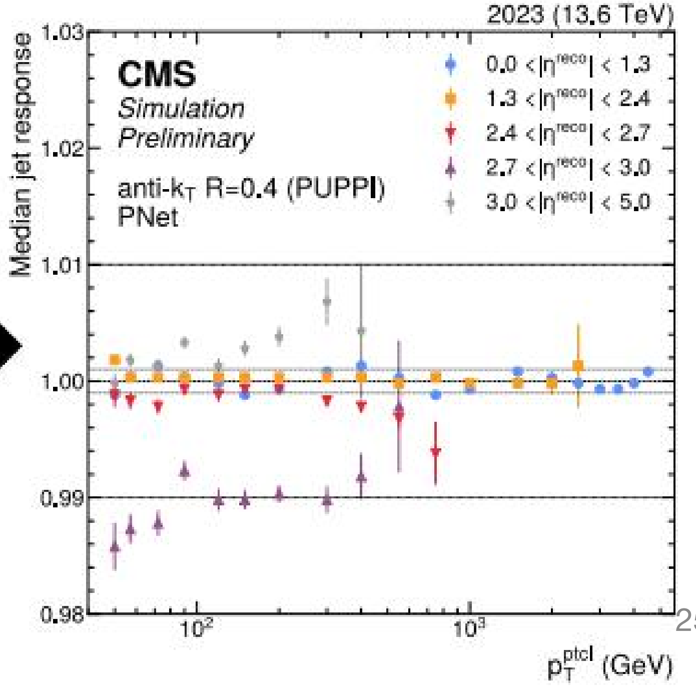

ParticleNet resolution

DP-2024-064

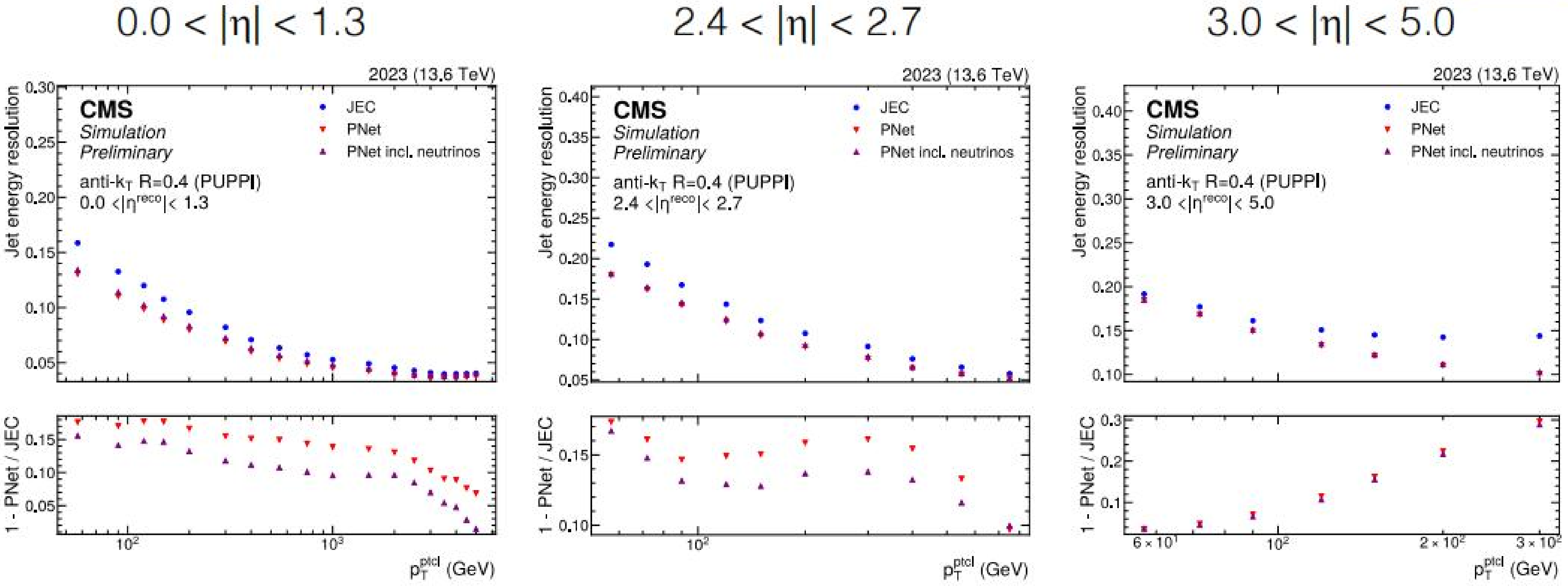

Clear improvement in JER
across the jet p_T range, even for forward jets.

Jet tagging

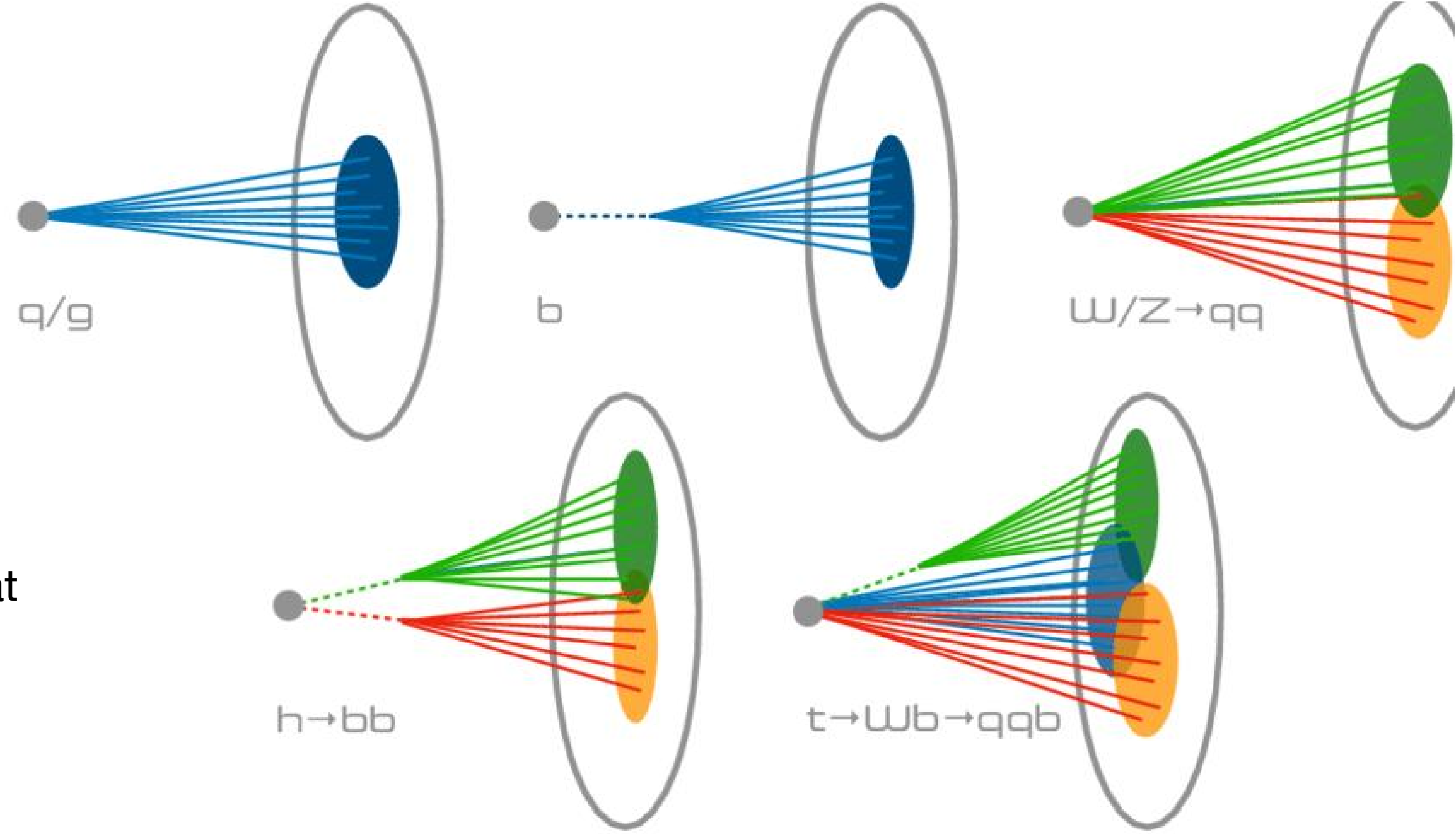

Tagging b-jets using impact parameter or secondary vertex as old as precision silicon tracking (or even older)

Tagging jets using its substructure started at the LHC due to the large boost that even massive particles can reach

Techniques evolved with time:

- physics-inspired variables
- combination of variables into MLP or DNN
- constituents into CNN (imaging), DNN or Transformers (ParticleNet)
- Lund Plane into GNN (LundNet)

At the same time, also b-tagging embraced Machine Learning

Graph Neural Network for Flavour tagging

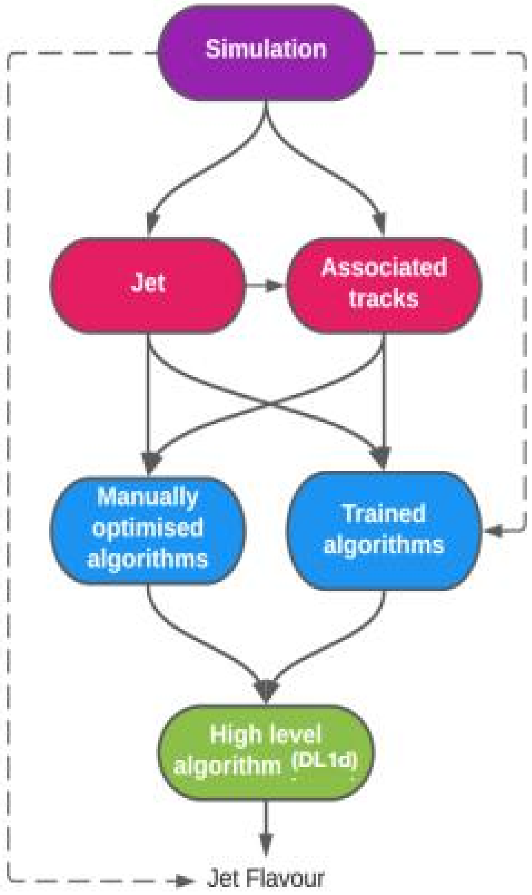

- **GN1** [ATL-PHYS-PUB-2022-027](): All-in-one GNN-based (Inspired by J. Shlomi's work -[arXiv:2008.02831]())
- Use track information and jet kinematics directly ⟹ naturally adapts to variable **#unordered input tracks**
- Tasks include **jet flavour, vertexing, and track origin prediction**, trained simultaneously
  - **Auxiliary targets enhance interpretability**
- Easily optimised for diverse use cases and track/jet improvements.

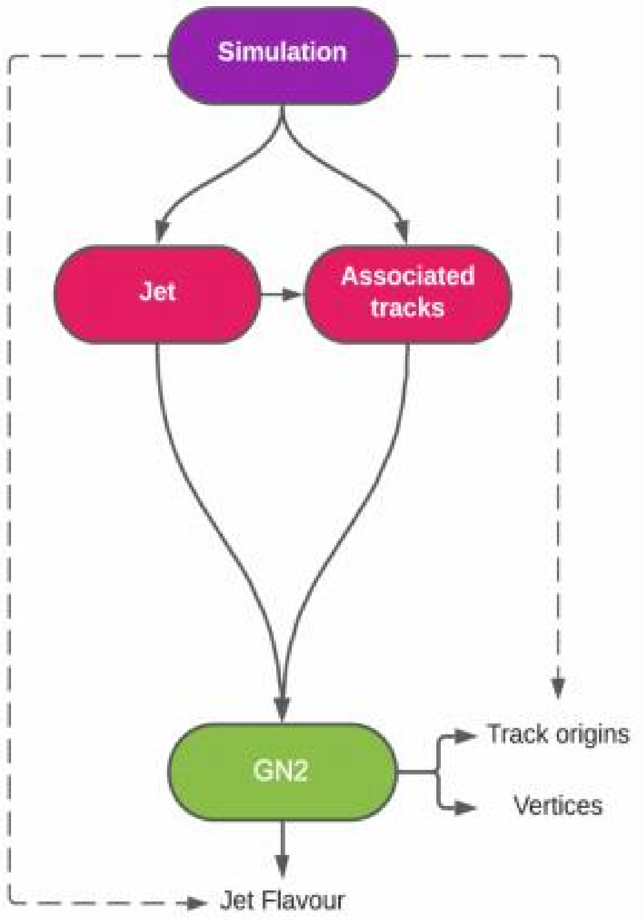

GN2 is an upgraded version of GN1: all-in-one transformer network with significant state-of-Art performance enhancements

GN2 is based on **GN1** architecture with **Optimised training , Updated architecture, Increased training statistics**

Architecture of GN2

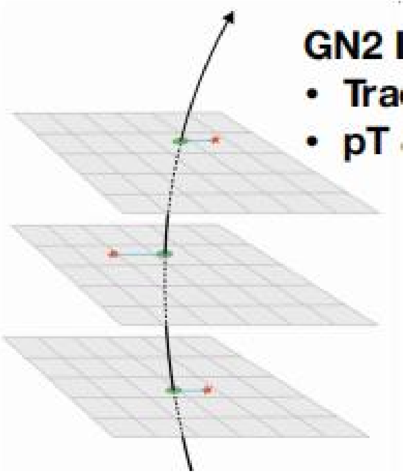

GN2 Inputs:
- **Tracks + jets variables**
- **pT & η resampled for each flavour**

Large Multimodal Multitask Transformer Model with over 2600k parameters (GN1: 800K, DL1d: 130k)

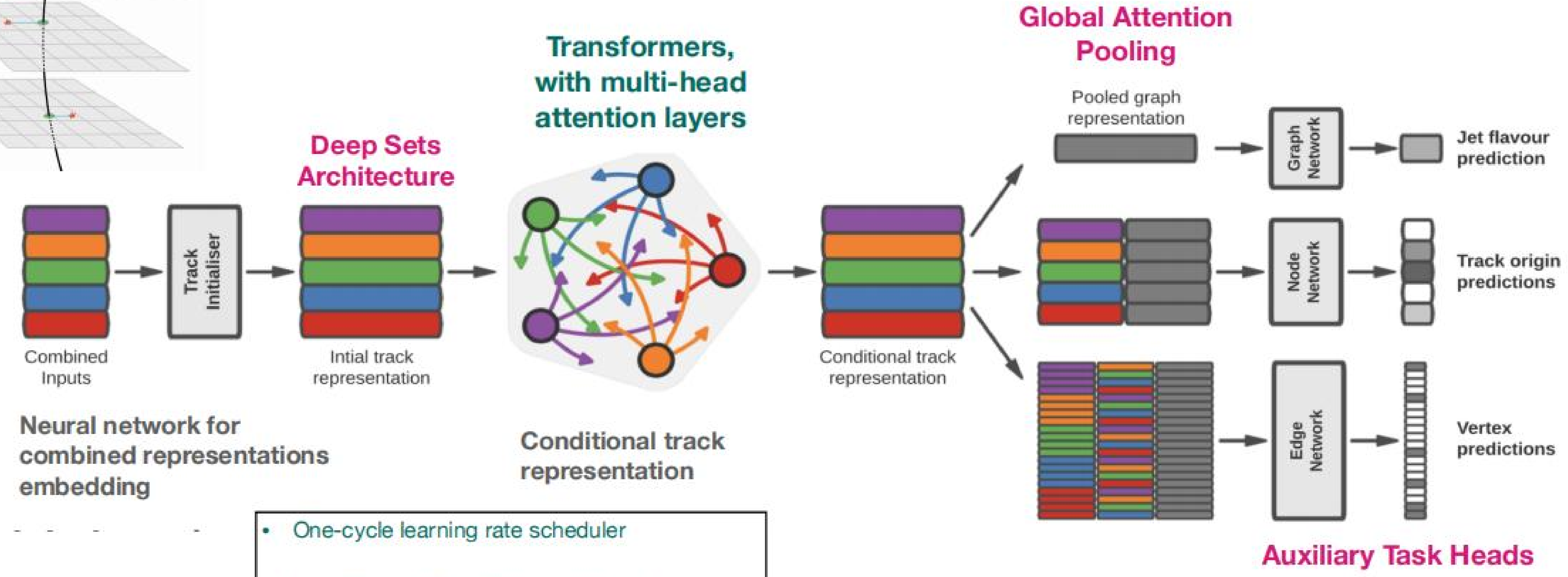

- One-cycle learning rate scheduler
- LayerNorm + DropOut to stabilise training
- Large training dataset: 192M training jets (GN2)

FTAG-2023-01

ATL-PHYS-PUB-2022-027

GN2 training performed using the Salt framework

Performance and future developments

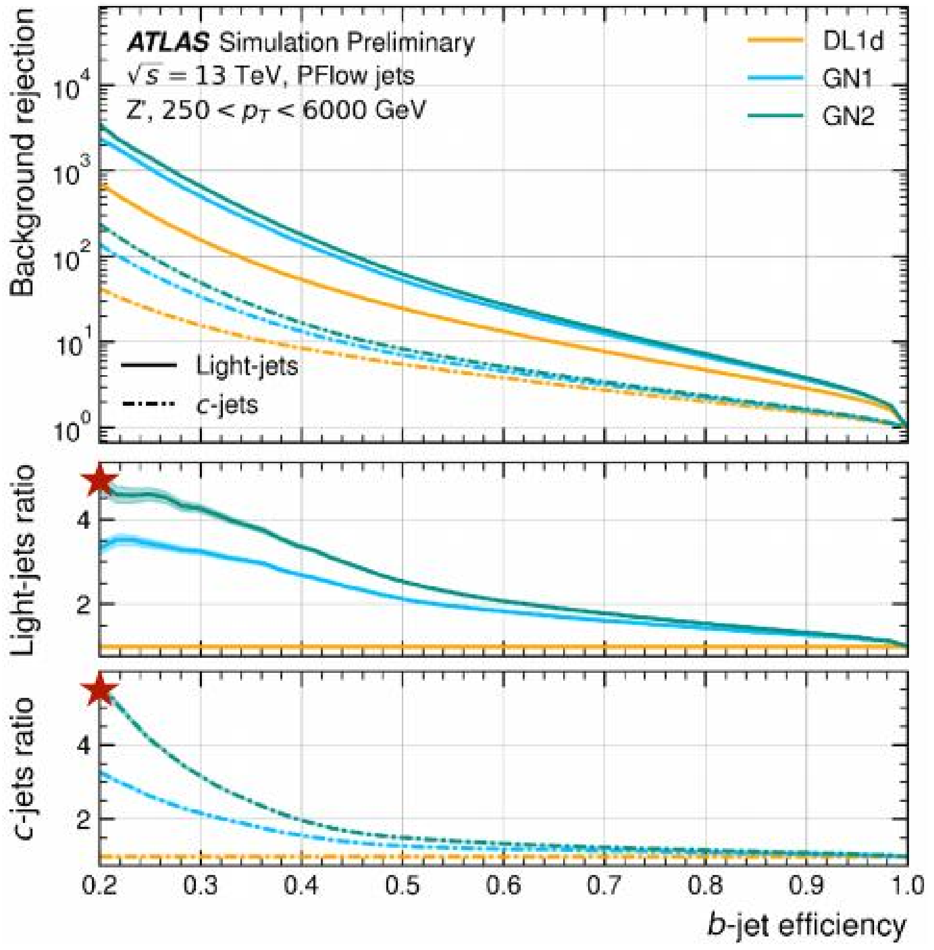

Better performance than any previous tagger

Transformer architecture can be used for other kinds of tagging, vertexing, trigger etc.

Double b-tagging for boosted jets in CMS

ParticleNet-MD state-of-art for CMS boosted jet tagging.

- Graph based architecture describing the jet as a particle cloud (unordered sample).

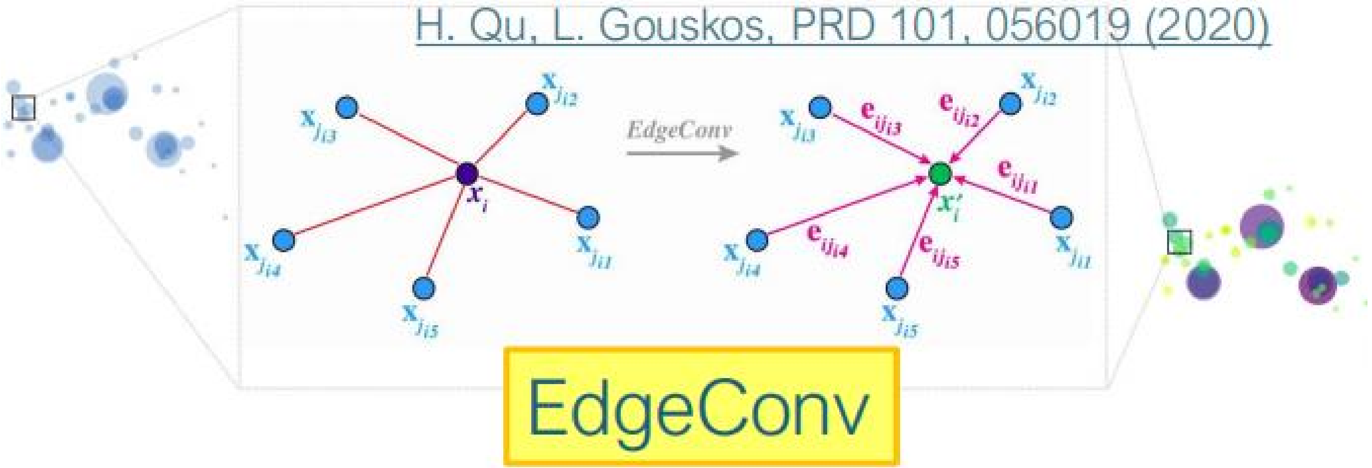

EdgeConv block:

- NN module part of the ParticleNet architecture;
- New features vector associated to each jet constituent and based on the features of the *k*-nearest neighbors.

Mass decorrelation:

- Trained on Monte Carlo (MC) simulations containing boosted resonances (X) with a flat distributions in both of p_t and mass, as the signal sample, and the QCD multijet sample (reweighted to yield flat distributions) as the background sample.

bb tagger evolution, architecture and performance

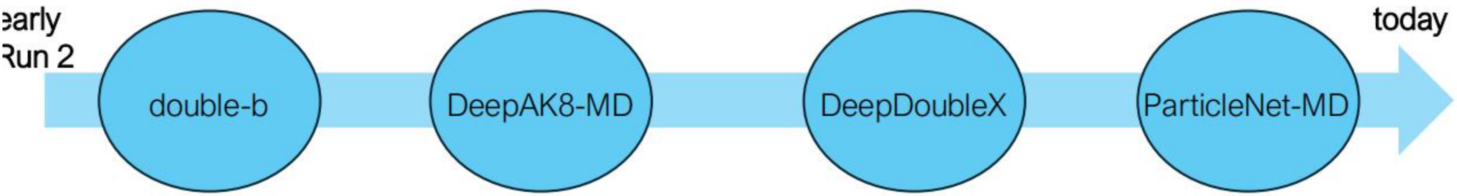

double-b

- Boosted Decision Tree (BDT)
- jet inputs: tracks and SVs
- output classes: H → b$\bar{b}$ vs QCD

DeepAK8-MD

- 1D Convolutional Neural Network (CNN)
- jet inputs: PF candidates and SVs
- output classes: X → b$\bar{b}$ vs QCD (bbvsQCD), X → c$\bar{c}$ vs QCD (ccvsQCD)

DeepDoubleX

- 1D CNN + Recursive NN
- jet inputs: PF candidates and SVs
- output classes: X → b$\bar{b}$ vs QCD (BvL), X → c$\bar{c}$ vs QCD (CvL), X → b$\bar{b}$ vs X → c$\bar{c}$ (BvC)

ParticleNet-MD

- Dynamic Graph CNN (DGCNN)
- jet inputs: PF candidates and SVs
- state of art for Run 3 CMS

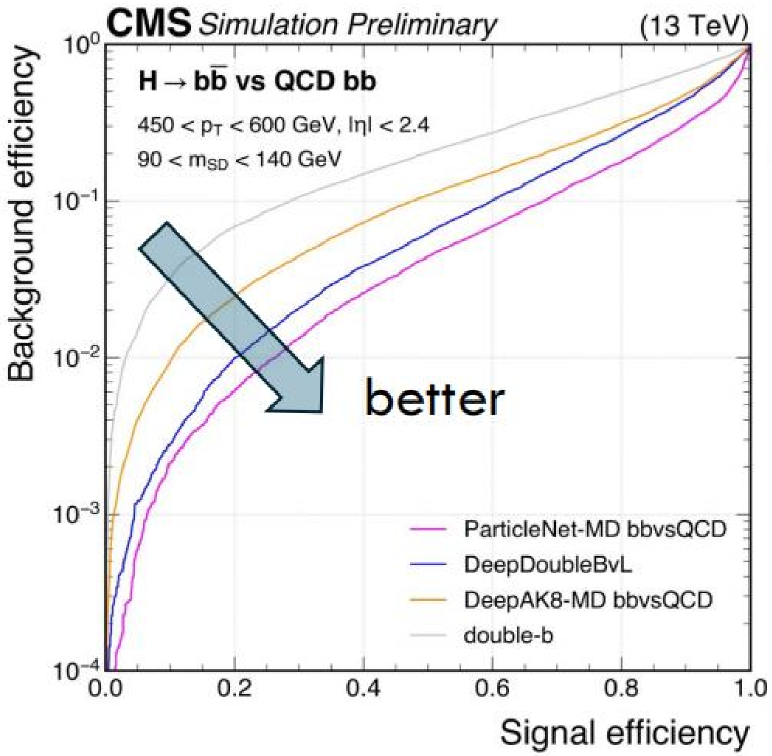

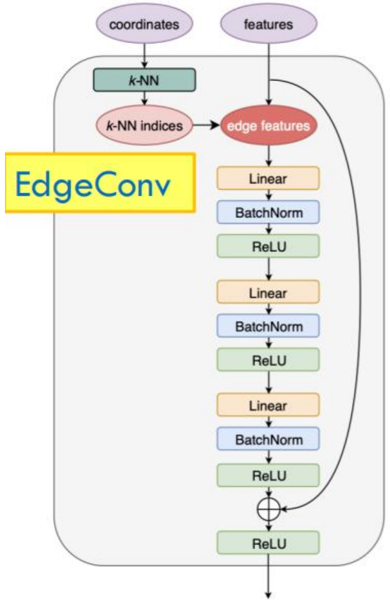

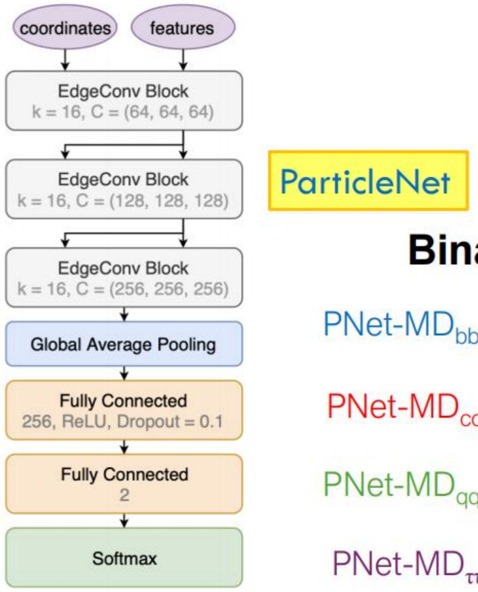

Binary outputs:

$$\text{PNet-MD}_{\text{bbvsQCD}} = \frac{p(X\to b\bar{b})}{p(X\to b\bar{b})+p(QCD)}$$

$$\text{PNet-MD}_{\text{ccvsQCD}} = \frac{p(X\to c\bar{c})}{p(X\to c\bar{c})+p(QCD)}$$

$$\text{PNet-MD}_{\text{qqvsQCD}} = \frac{p(X\to q\bar{q})}{p(X\to q\bar{q})+p(QCD)}$$

$$\text{PNet-MD}_{\tau\tau\text{vsQCD}} = \frac{p(X\to \tau\bar{\tau})}{p(X\to \tau\bar{\tau})+p(QCD)}$$

Boosted object tagging with substructure in the ML era

Machine-learning/pheno community is developing faster then we can test on data!

- Normal dense neural networks
- ResNet: CNN Architecture representing jet as image
- Energy/Particle Flow networks (EFN/PFN): General decomposition of IRC-safe observables
- ParticleNet: Graph network on point cloud
- ParticleTransformer: Transformer
- GN2X: Transformer with auxiliary tasks
- LundNet: Graph on declustering history
- PELICAN: Lorentz invariant network

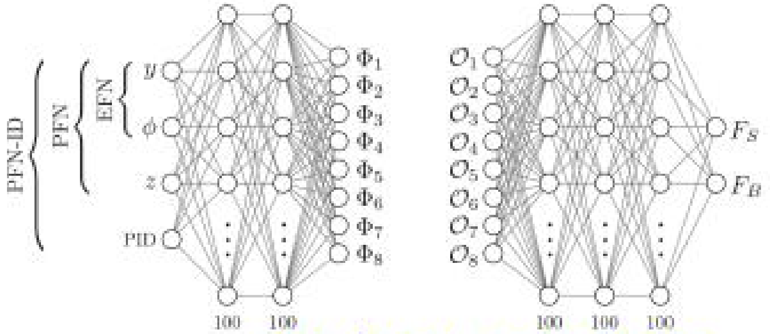

EFN/PFN: 1810.05165

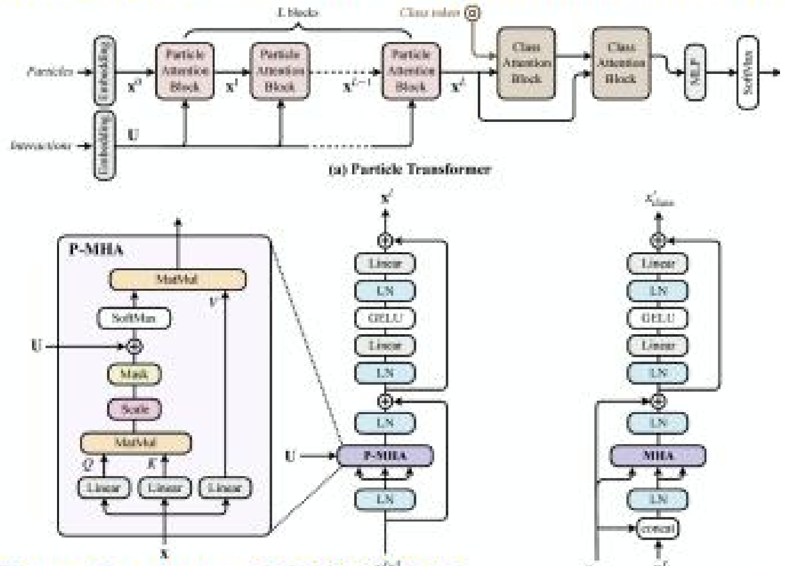

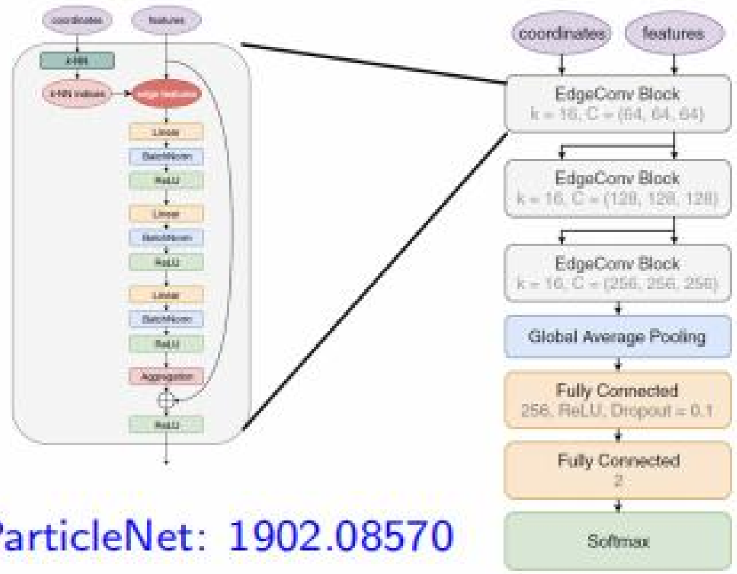

ParticleTransformer: 2202.0377

ParticleNet: 1902.08570

DNN tagger in ATLAS ATL-PHYS-PUB-2021/28-29

Baseline DNN top-taggers / W-tagger at $50/80\%$ signal efficiency over 15/10 substructure observables

- Factor $\sim$1.6/6 gain for W/top-tagging vs single substructure variable

Tagger performance deeply connected to jet definition!

- Over Run2 moved from calorimeter $\rightarrow$ calorimeter+tracking information
- Factor 2 gains in background rejection
  - Due to better mass+substructure resolution

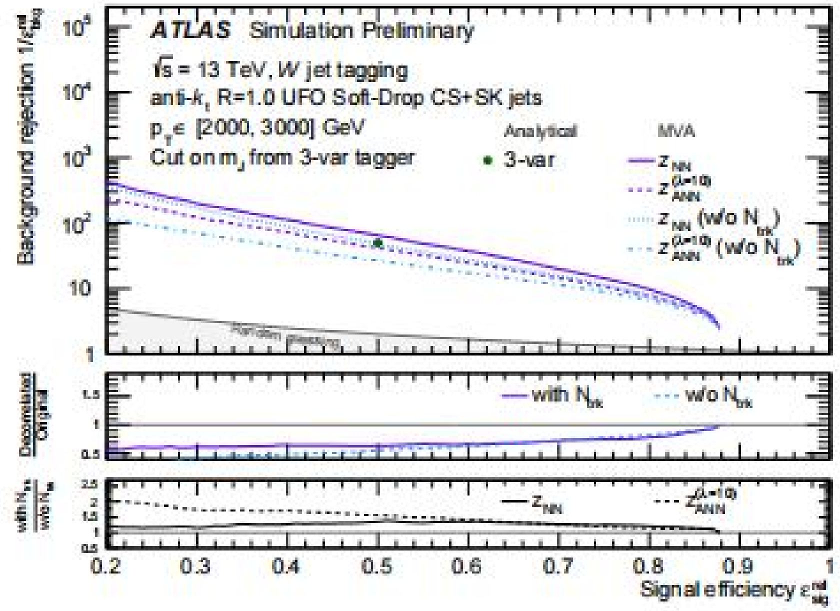

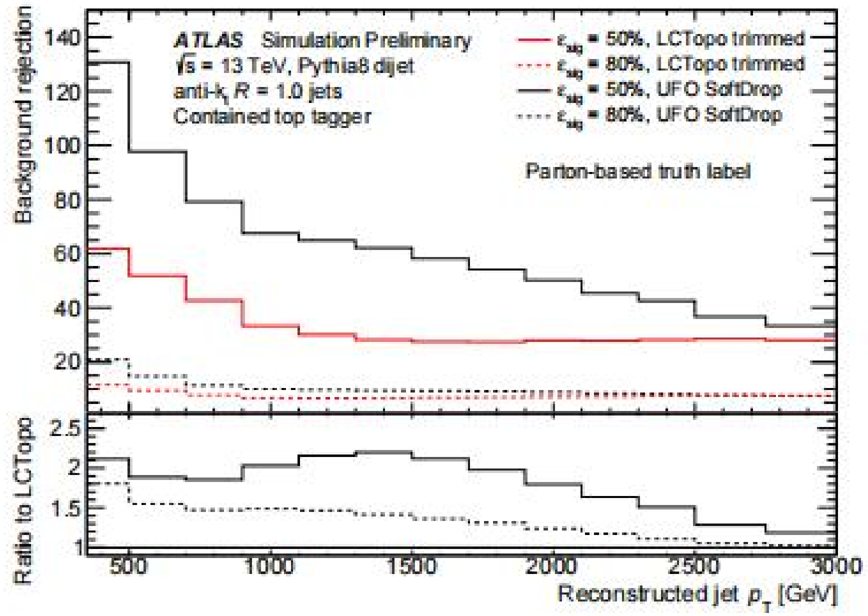

Constituent-based taggers ATL-PHYS-PUB-2021-039/2023-020

Constituent based top-tagger / W-tagger outperform high-level features ones:

- Provide network the lowest level information available: the jet constituents themselves
- Another factor 2-3 improvement!
- ResNet/EFN under-perform w.r.t theoretical performance
  - Real simulation studies important!

top-tagger ROC

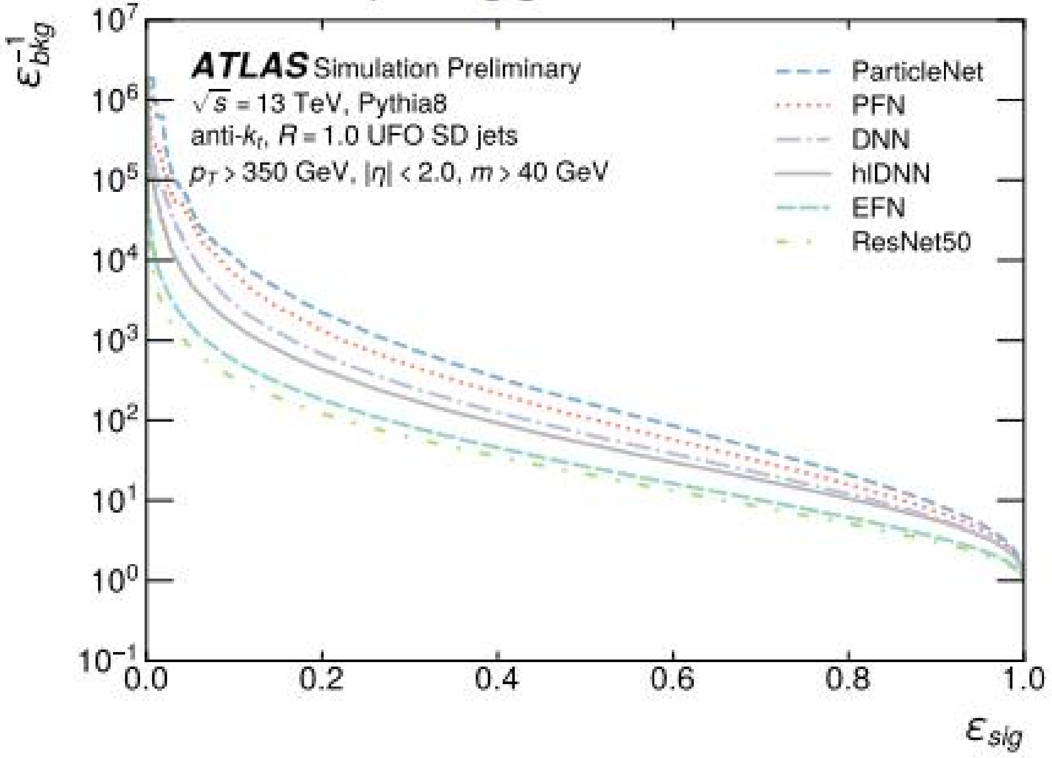

W-tagging summary table

Model	AUC	ACC	ϵ_{bkg}^{-1} @ ϵ_{sig} = 0.5	ϵ_{bkg}^{-1} @ ϵ_{sig} = 0.8	# Params	Inference Time
EFN	0.920	0.835	35.1	7.95	56.73k	0.065 ms
PFN	0.931	0.853	44.7	9.50	57.13k	0.11 ms
ParticleNet	0.933	0.826	46.2	9.76	366.16k	0.36 ms
ParticleTransformer	0.951	0.880	77.9	14.6	2.14M	0.28 ms

(A parenthesis: the Lund Jet Plane)

- Idea: reconstruct distribution of QCD radiation inside jet by constructing Lund Planes from proto-jets in CA algorithm.
- To reconstruct: calculate kinematic variables, eg

$$z = \frac{p_T^e}{p_T^e + p_T^c}; \qquad \Delta R = \sqrt{(y_e - y_c)^2 + (\phi_e - \phi_c)^2}; \qquad k_t = p_T^e \Delta R,$$

  for proto-jets e, c in each step where $p_T^e < p_T^c$.

- Plot LJP for angular + momentum variable. (Total number of emissions) / (total number of jets) gives the average emission density ρ_{LJP}.
- These *Lund Jet Planes* [Dreyer, 1807.04758] have many interesting features. Radiation of different origins is factorised across the plane.
- LJP relates closely to other jet substructure observables that are built from CA clustering sequences, e.g. the *Soft Drop* [Larkoski, 1402.2657,ATLAS, 1912.09837] jet mass which show similar behaviour.
- To leading order in QCD, the emission density is proportional to $\alpha_s(k_t)$.

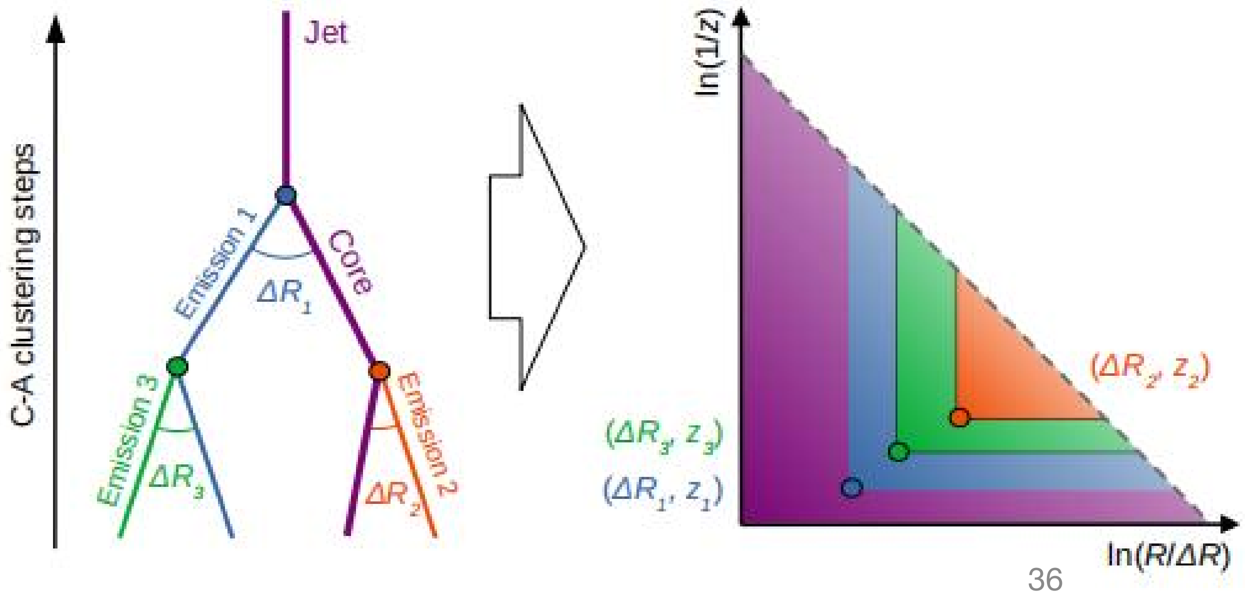

Why is the LJP impotant in QCD?

- Emissions of different scales and origins enter in different regions of the plane

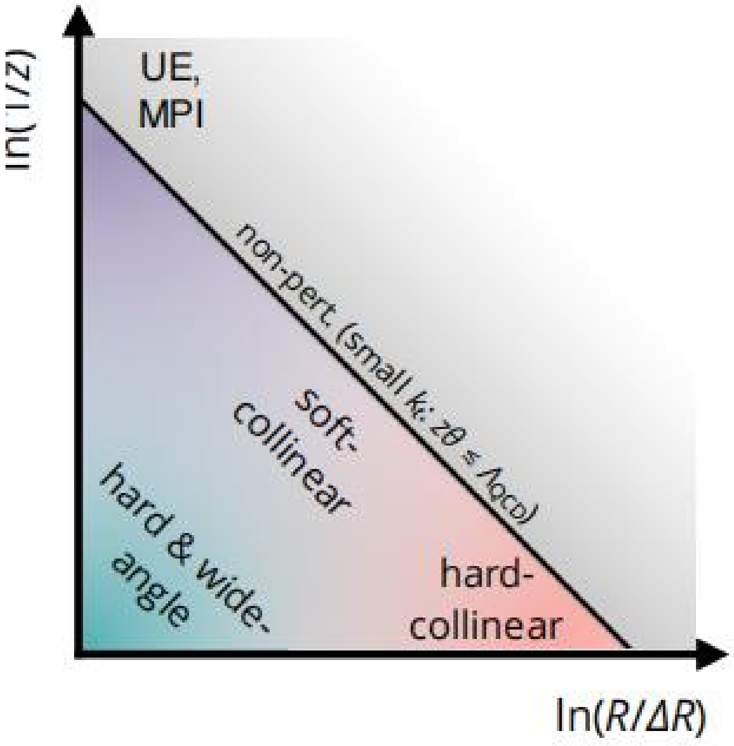

Parton shower

(Ang. ord. / Dipole)

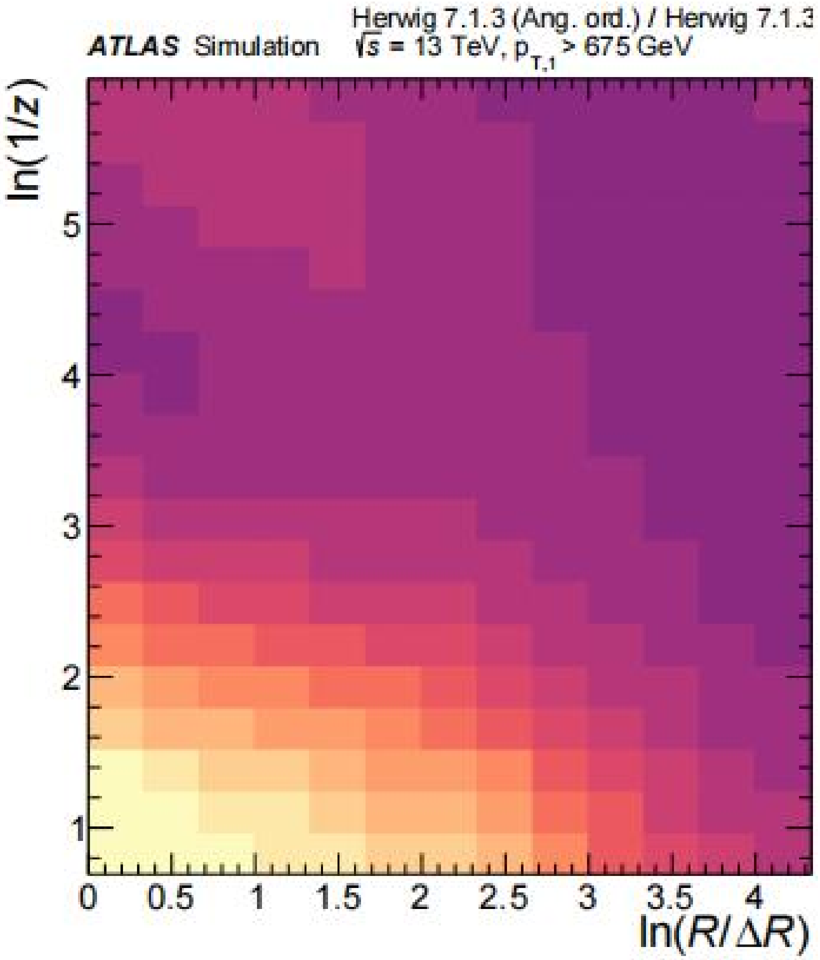

Hadronization

(Lund string / AHADIC)

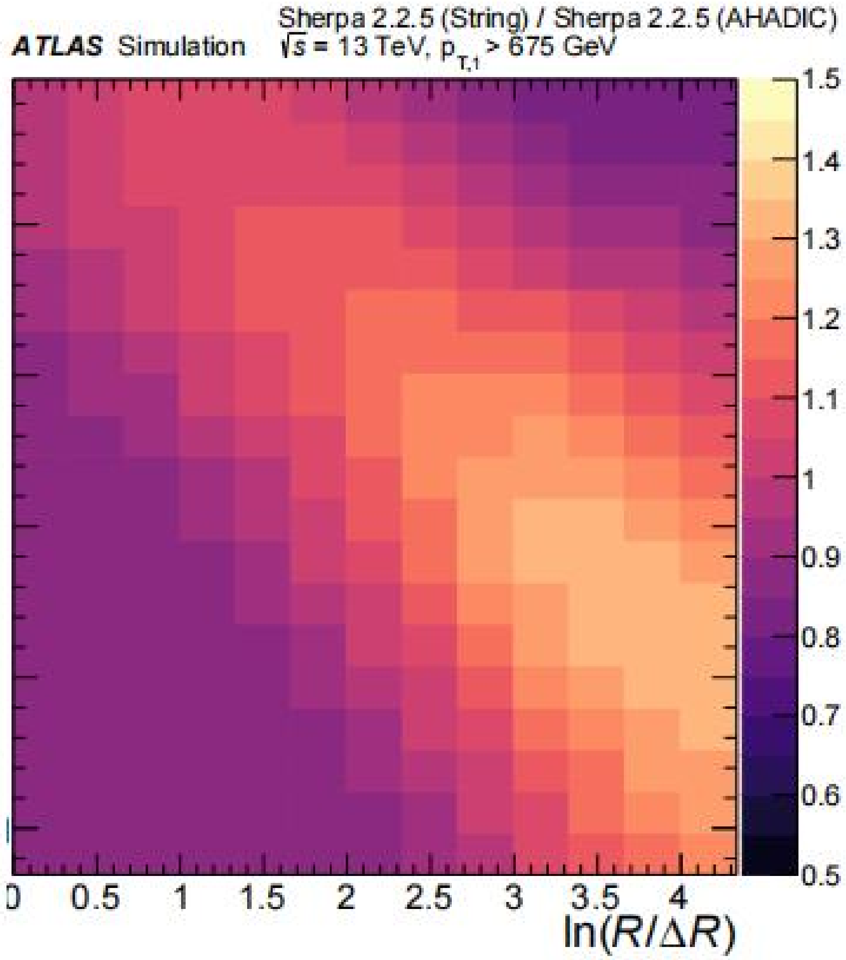

Ratios between MonteCarlos:
Different PS

Source: EP-2020-030

Different Hadronisation

Using the LJP as a Physics-aware tagger

- The distinctive features of the LJP make it an interesting observable for jet tagging.
- Wide-angle splittings due to heavy particle decays clearly visible in the LJP. Quark and gluon jets can also be distinguished [Dreyer, 2112.09140].
- Can apply different types of neural networks to take advantage of these input shapes eg. conv. nets [Oliveira, 1511.05190], LSTMs [Dreyer, 1807.04758].
- Latest developments: graph neural networks [Dreyer, 2112.09140, Qu, 1902.08570] using the LJP coordinates on the full CA clustering tree as input features
- *LundNet* uses EdgeConv [Wang, 1801.07829] layers to perform convolutions along edges of graphs.

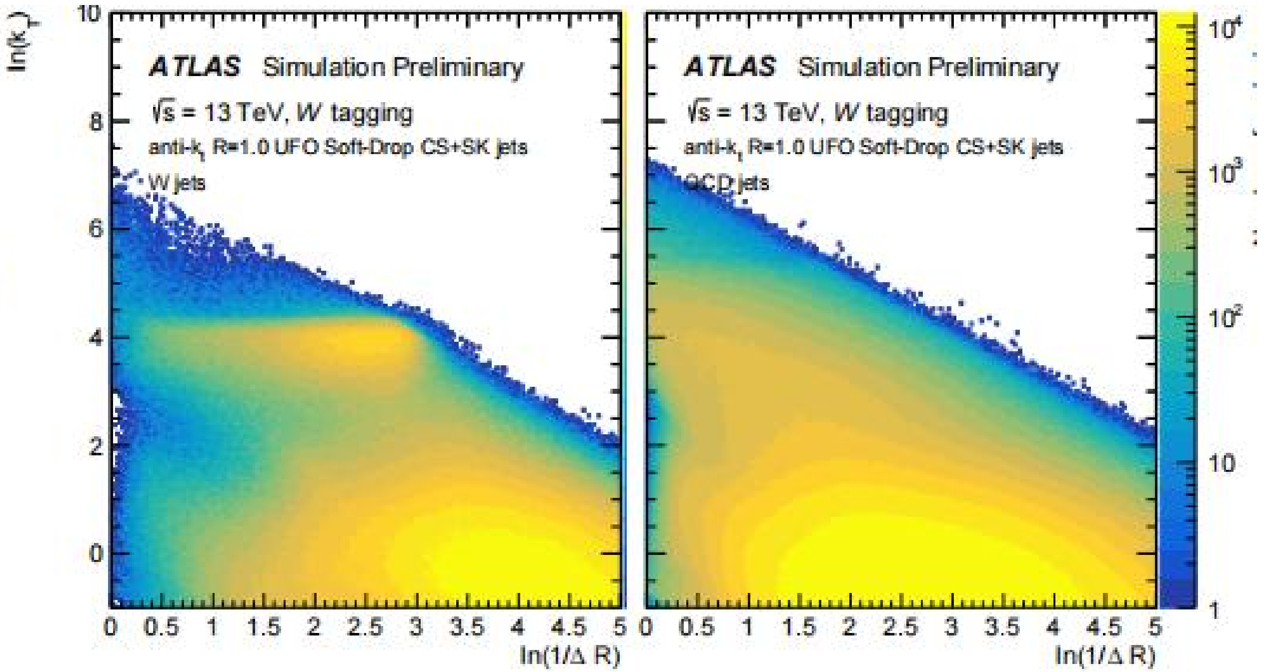

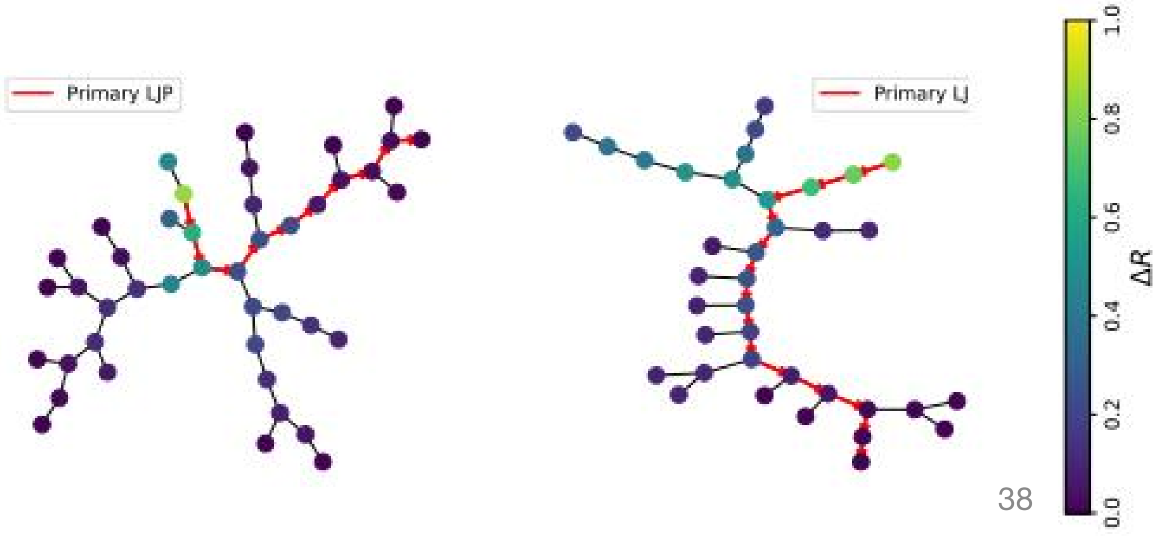

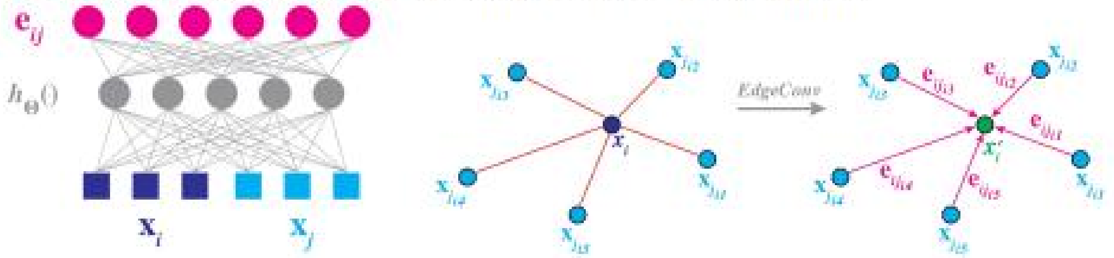

Comparison of W and Top taggers in ATLAS

The more information you feed into the network, the better the network classification power will be

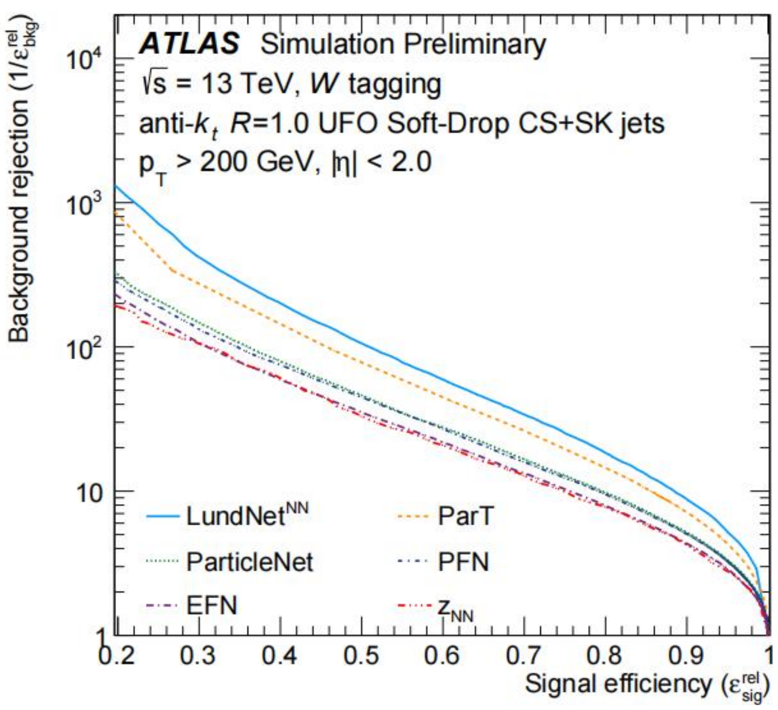

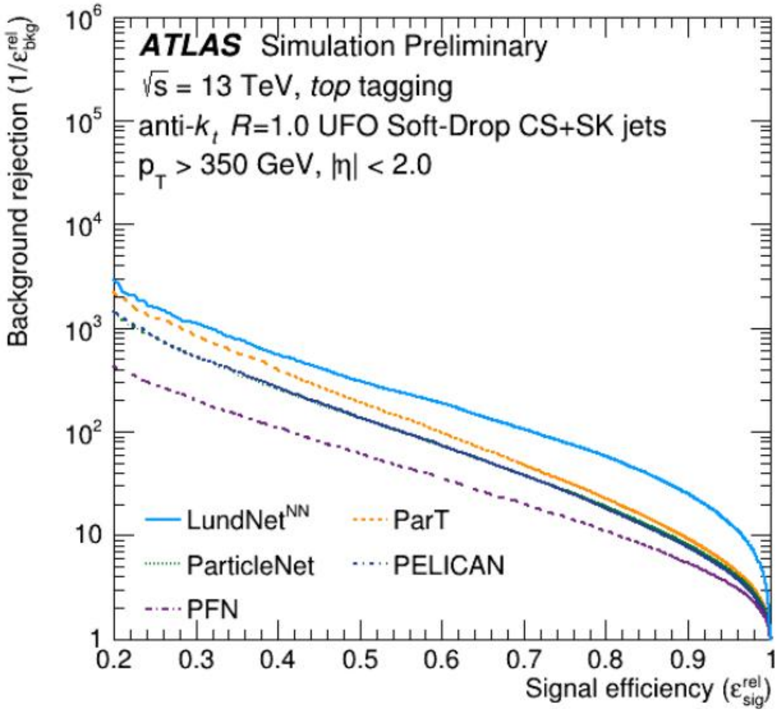

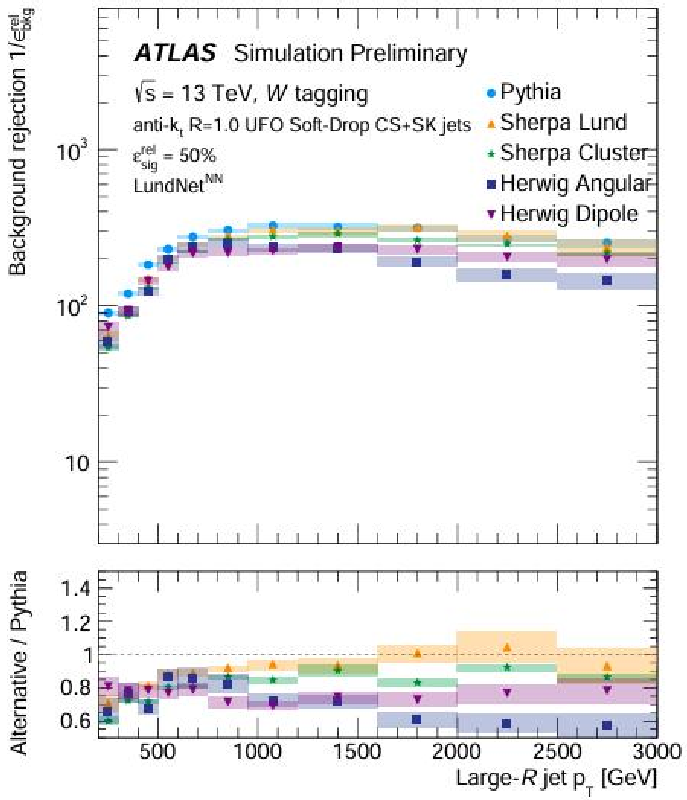

However, the most sophisticated the tagger, the larger will be the modeling systematics

Can have > 20% difference in performance using a MC model different from the one used for training

Working to mitigate it (adversarial networks, mixed training, training on data, cutting away LJP etc.)

Tagger comparison in CMS CERN-EP-2020-037 2020/06/09

substructure variables

Heavy Objects Variable R Tagger

Energy Correlation

Boosted Event Shape

CNN imaging

“Particle “and “Vertex” lists into a DNN

Algorithm	Subsection	jet p_T [GeV]	t quark	W boson	Z boson	H boson
$m_{SD} + \tau_{32}$	6.1	400	✓			
$m_{SD} + \tau_{32} + \mathrm{b}$	6.1	400	✓			
$m_{SD} + \tau_{21}$	6.1	200	✓	✓		
HOTVR	6.2	200	✓			
N_3-BDT (CA15)	6.3	200	✓			
$m_{SD} + N_2$	6.3	200		✓	✓	✓
BEST	6.5	500	✓	✓	✓	✓
ImageTop	6.6	600	✓			
DeepAK8$^{(*)}$	6.7	200	✓	✓	✓	✓
Jet mass decorrelated algorithms						
$m_{SD} + N_2^{DDT}$	6.3	200		✓	✓	✓
double-b	6.4	300			✓	✓
ImageTop-MD	6.6	600	✓			
DeepAK8-MD$^{(*)}$	6.7	200	✓	✓	✓	✓

mostly multi-class taggers combining b-tagging and substructure

Taggers performance on MC

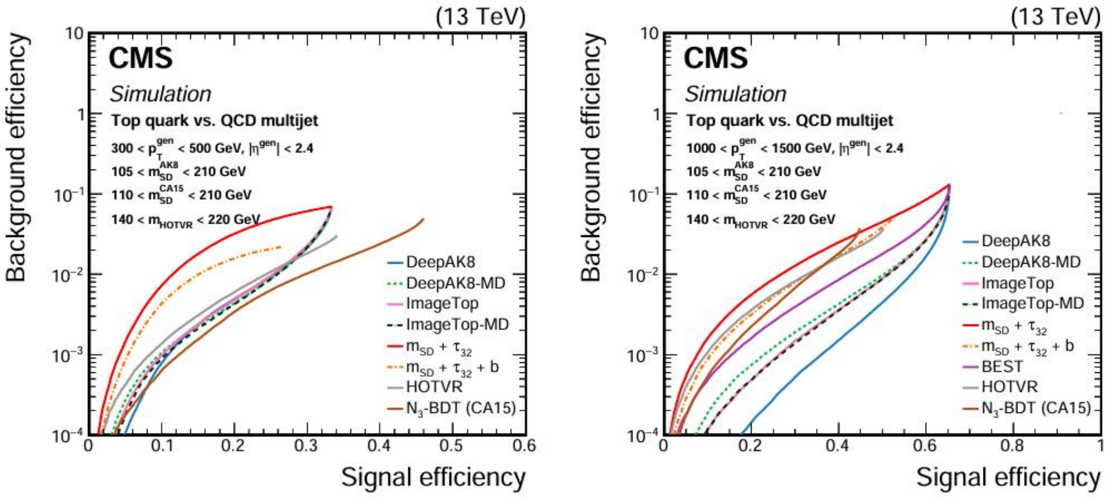

top vs QCD

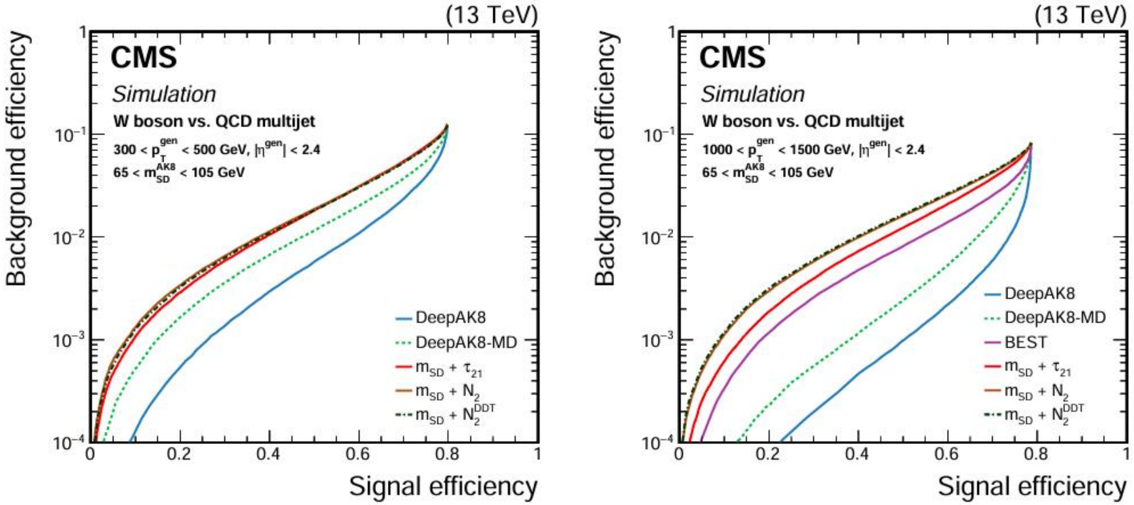

W vs QCD

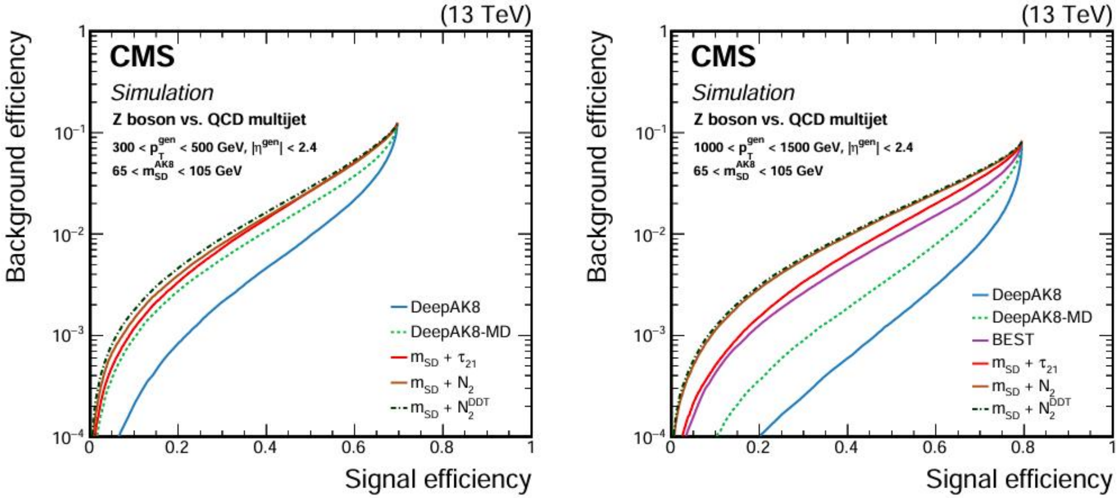

Z vs QCD

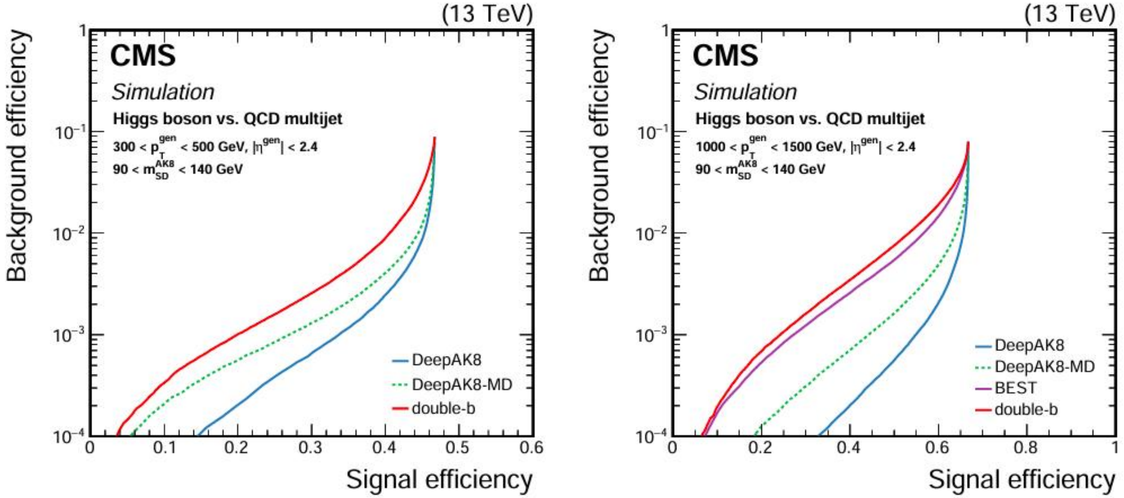

Higgs vs QCD

Deep AKT8 architecture

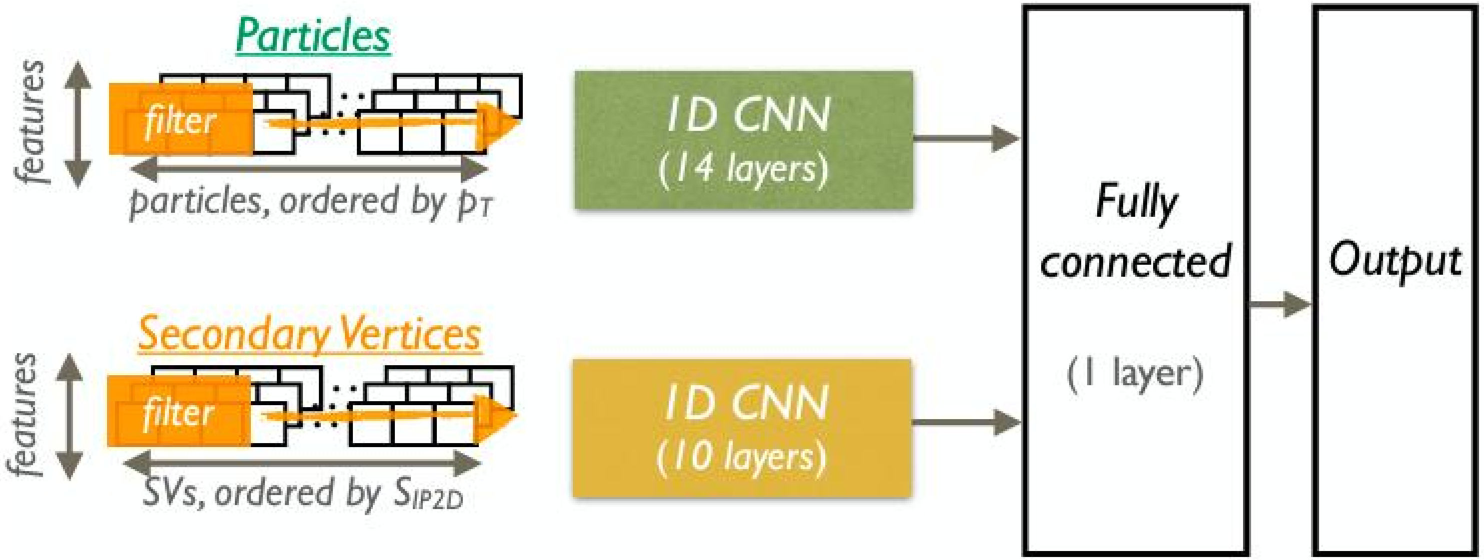

Use CNN to reduce dimentionality and extract features from list of particles and secondary vertices

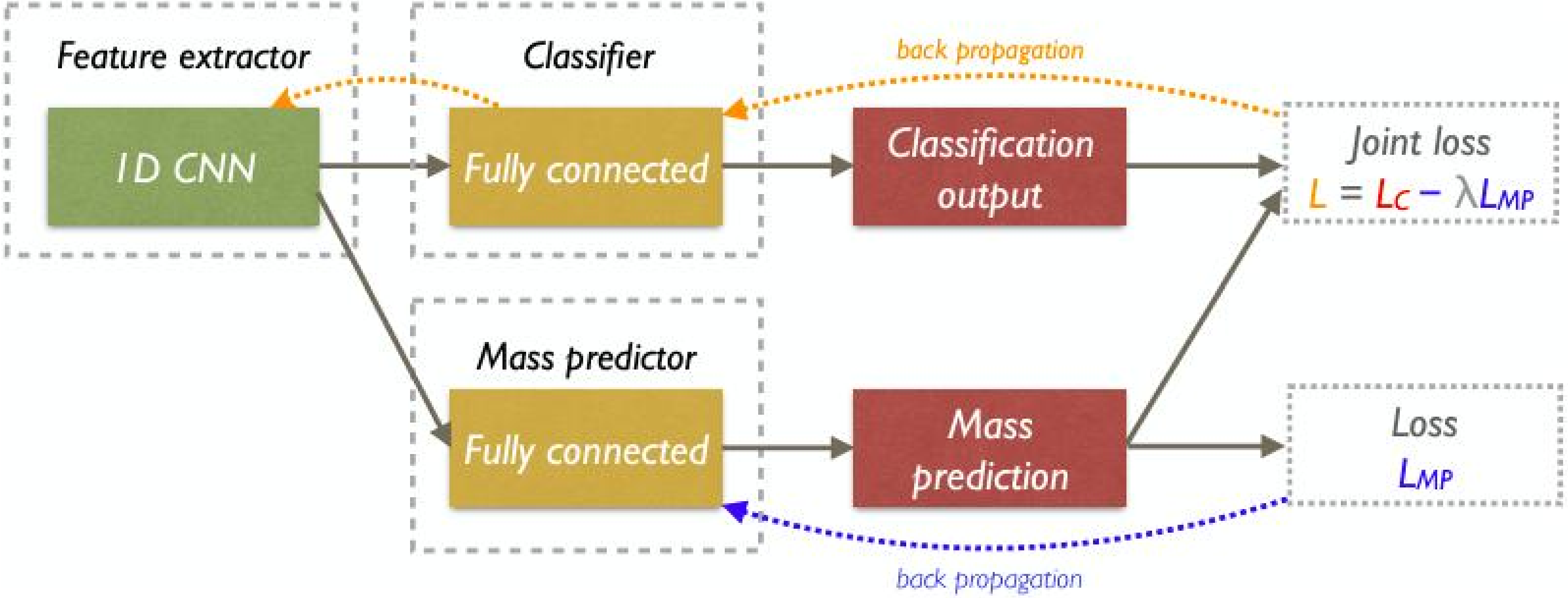

Mass-decorrelated version has a mass predictor that can be used in the loss function to avoid shaping the BG around the signal mass

Variable- Radius top taggers

Heavy Object Tagger with Variable Radius

- $R = 600 / p_t$ (R min 0.1, R max 1.5).
- Useful for 4 top final states where the top quark is not completely boosted ($200 < p_t < 800$ GeV).
- Efficiency as the ratio between the generated top quarks matching a reconstructed jet within ΔR and all the generated top quarks.

Developed a BDT to distinguish top quarks from QCD:

- Training on QCD multijet and the ttZ to simulate the background and the signal, respectively;
- Tested on a Z+jets enriched selection
  - Two opposite sign leptons ($80 < m_{\ell\ell} < 101$ GeV) + >1 HOTVR

CMS-DP-2024-038

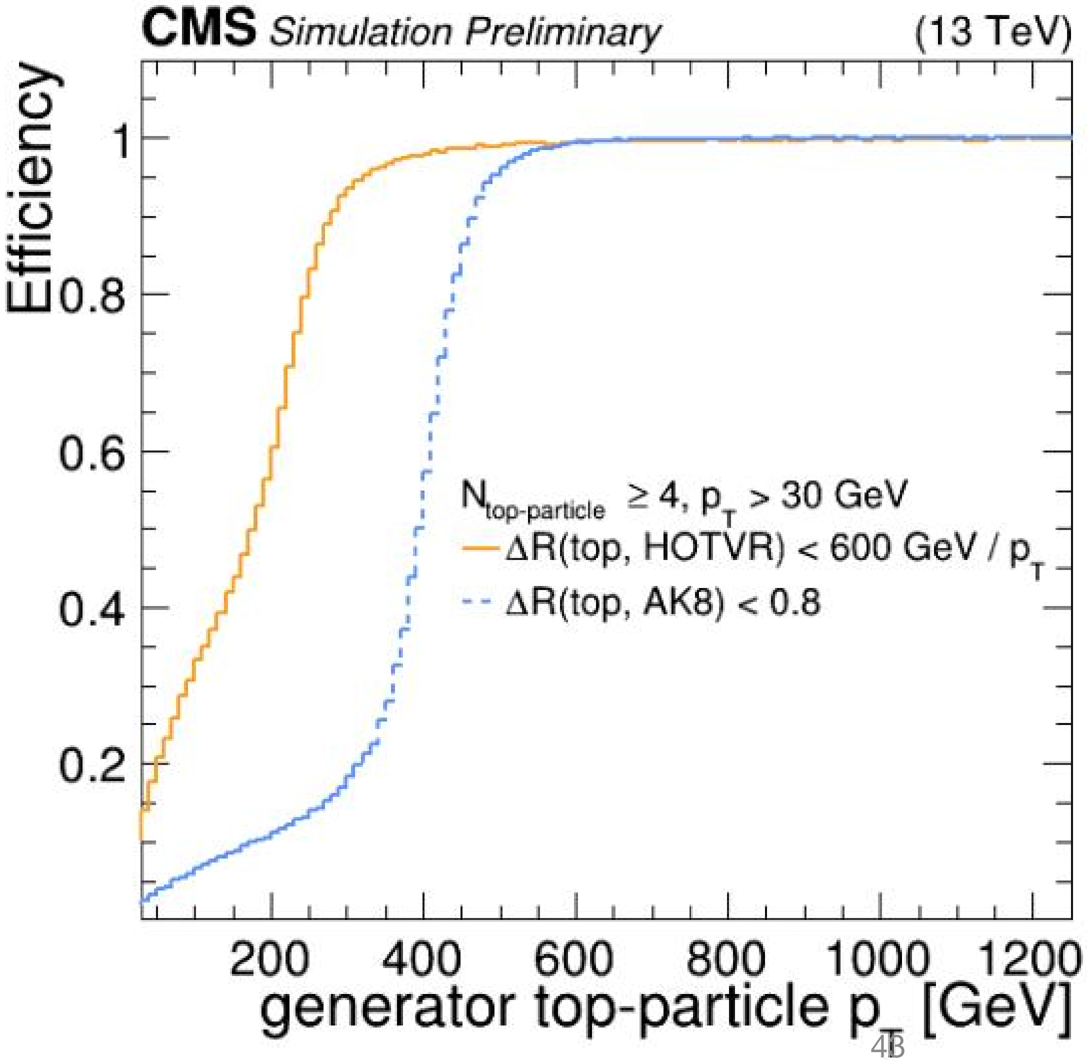

Measuring substructure: the Lund Jet Plane for dijets

- First ever measurement of the Lund Jet Plane observable by ATLAS in dijet events [EP-2020-030].
- Uses the full ATLAS Run 2 dataset with lowest p_T un-prescaled single jet triggers. More than 29 million jets!
- Jets are reconstructed from calorimeter topoclusters using anti-k_T with $R = 0.4$.
- Event selections:
  - 2 jets, both $|\eta| < 2.1$
  - $p_T^{\text{leading}} > 675\,\text{GeV}$
  - Dijet balance: $p_T^{\text{leading}} < 1.5 \times p_T^{\text{sub-leading}}$
- LJPs are reconstructed for both jets. High jet p_T ensures good LJP resolution.
- Measurement was later compared to all-orger NLL resummations [Lifson, 2007.06578]. Good overall agreement, mismodelling at jet boundary due to CA-reclustering of anti-k_t jet.

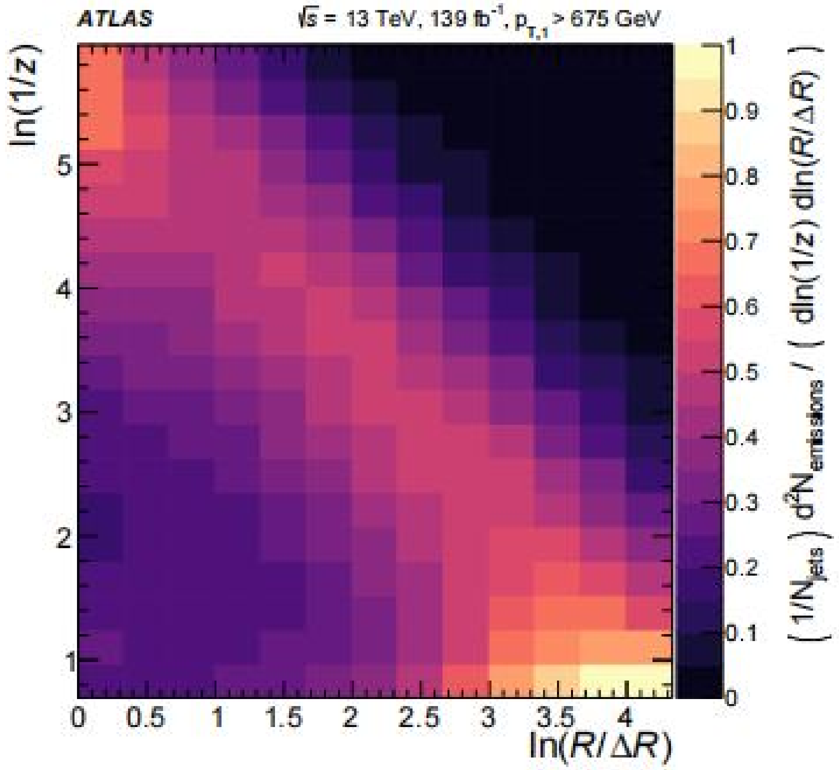

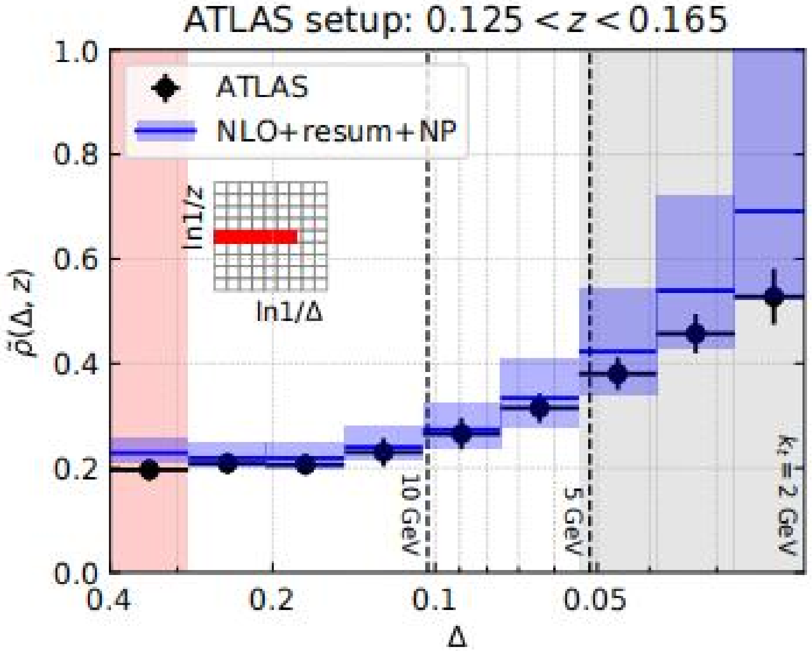

Running of αs in a single jet, and analytical comparisons

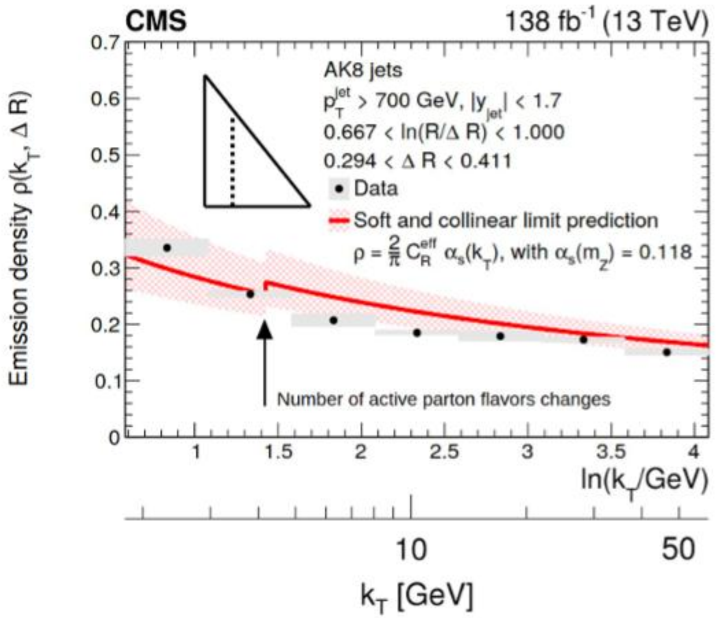

Recall LO pocket formula for Lund density:

$$\frac{1}{N^{\mathrm{jets}}} \frac{\mathrm{d}^2 N_{\mathrm{emissions}}}{\mathrm{d}\ln(k_T)\mathrm{d}\ln(R/\Delta R)} \simeq \frac{2}{\pi} C_R \alpha_s(k_T)$$

Running $\alpha_S(k_T)$ from few GeV to ~60 GeV qualitatively describes the data
(Assuming q/g fractions from PYTHIA8)

Cute to see, but breaks down
at large angles ΔR, close to the edge, etc

Calculations from A. Lifson, G. Salam, G. Soyez [JHEP10(2020)170]

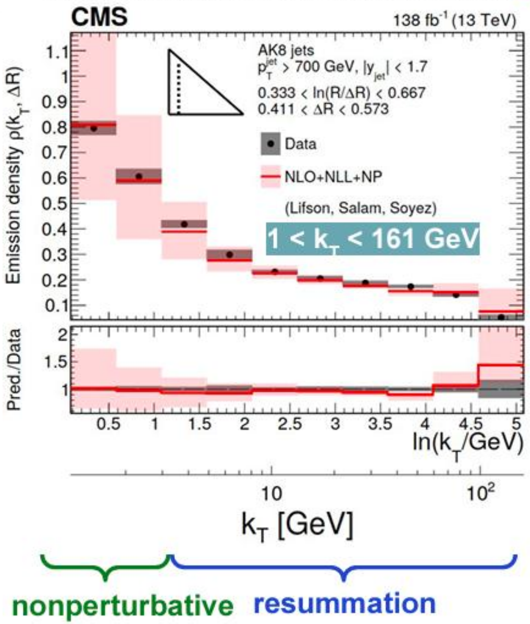

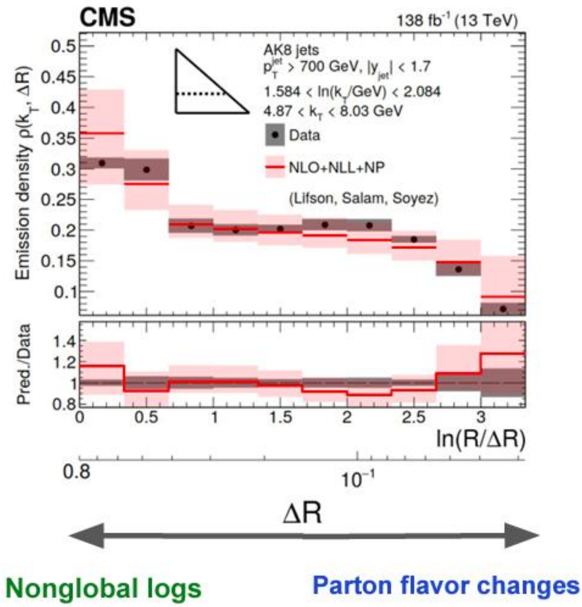

Lund Jet Plane for W and Top jets

- LJPs for Top jets and *W* jets are presented separately.
- Unfold LJP to the particle level using Iterative Bayesian Unfolding with 4 iterations.
- Structure related to the top/W mass is observed in the lower-left corner of the LJP
- Unfolded distributions of the LJP are compared to a wide range of alternative $t\bar{t}$ MC configurations.
- Results could be useful for tuning $t\bar{t}$ MCs or developing and calibrating (see CMS-DP-2023-046) heavy particle jet taggers. $t\bar{t}$ events could also be investigated in future to measure LJP for b jets.

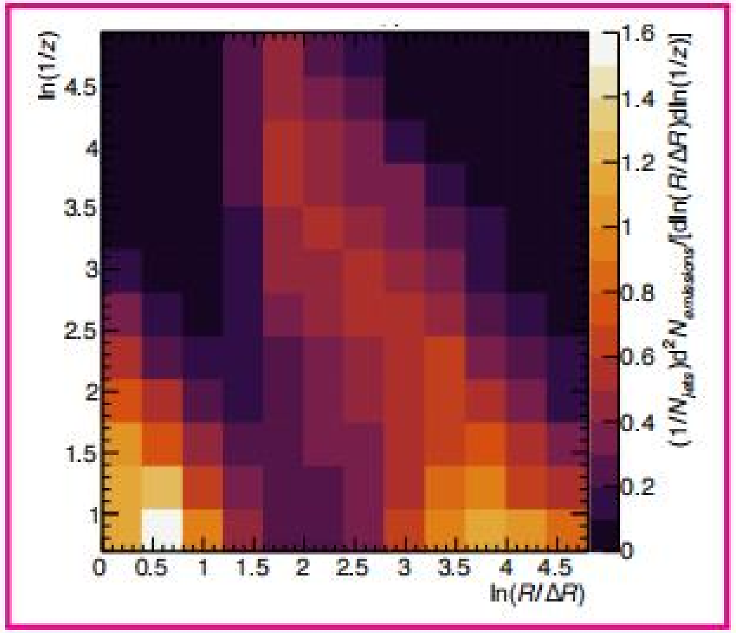

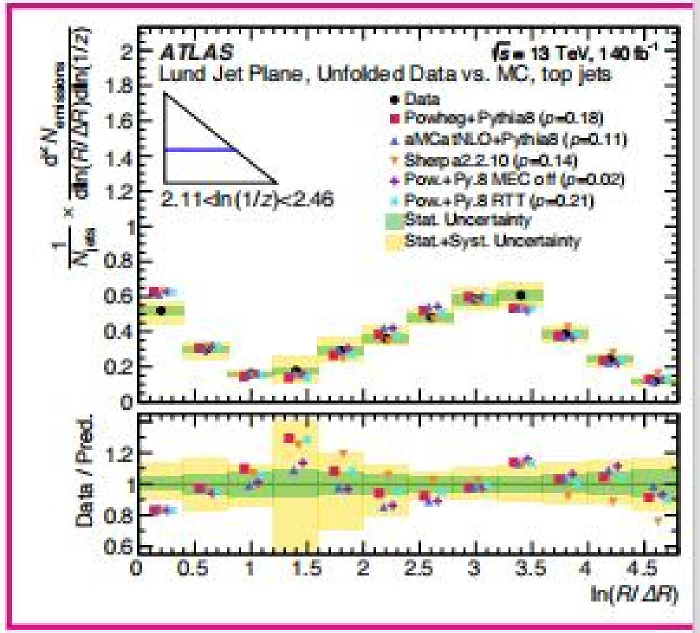

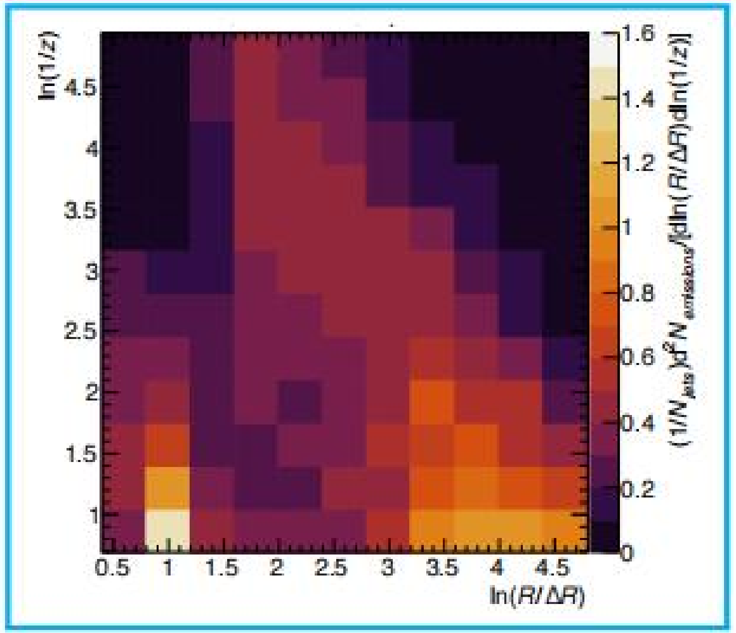

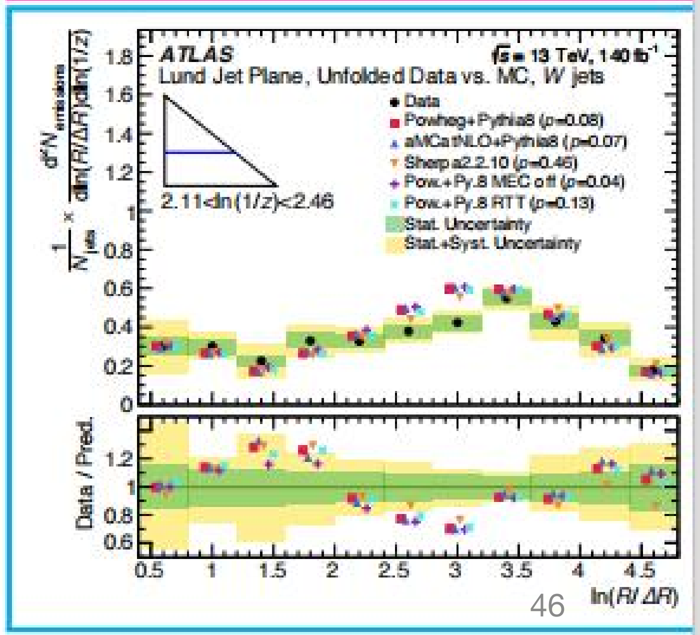

Using jet tagging for searches

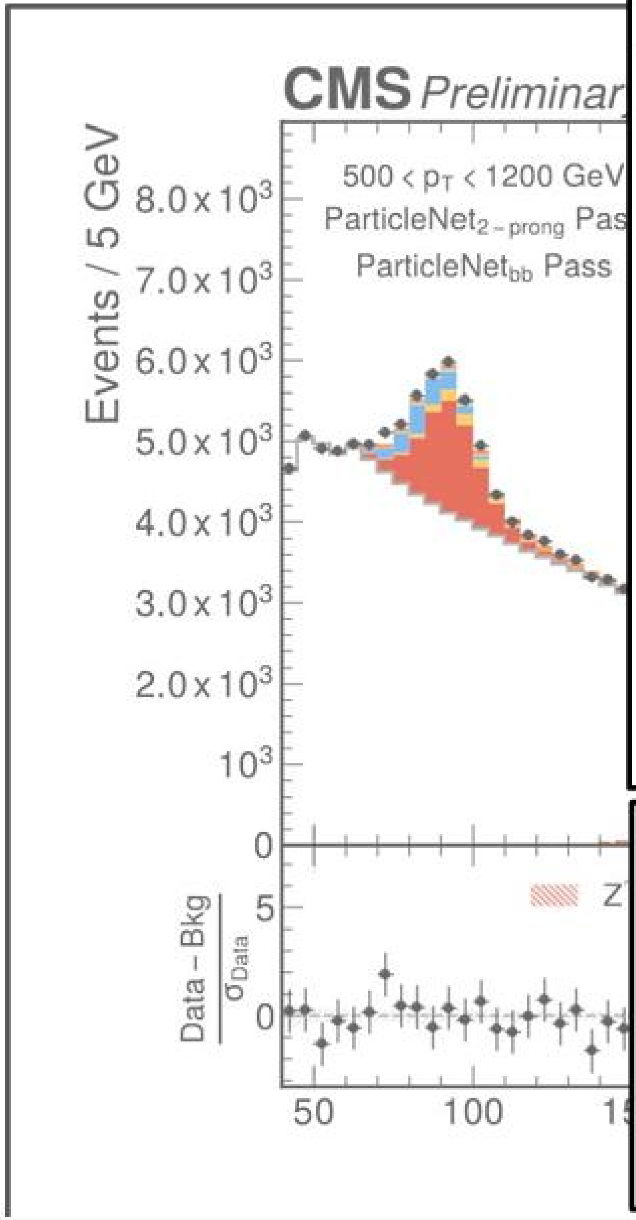

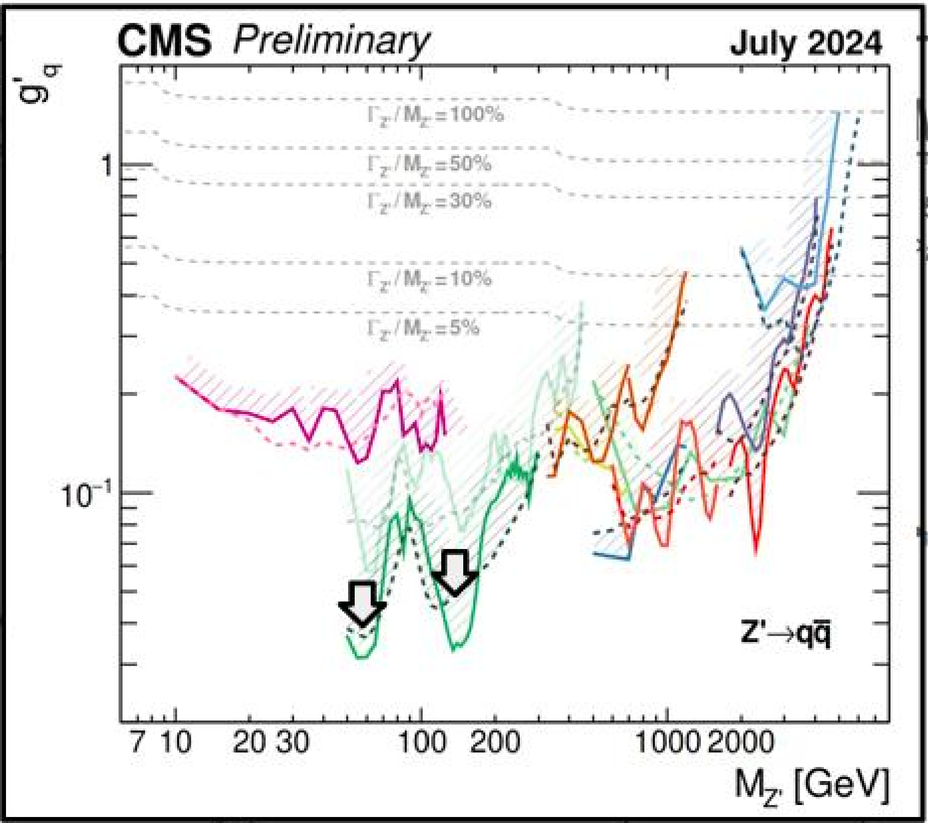

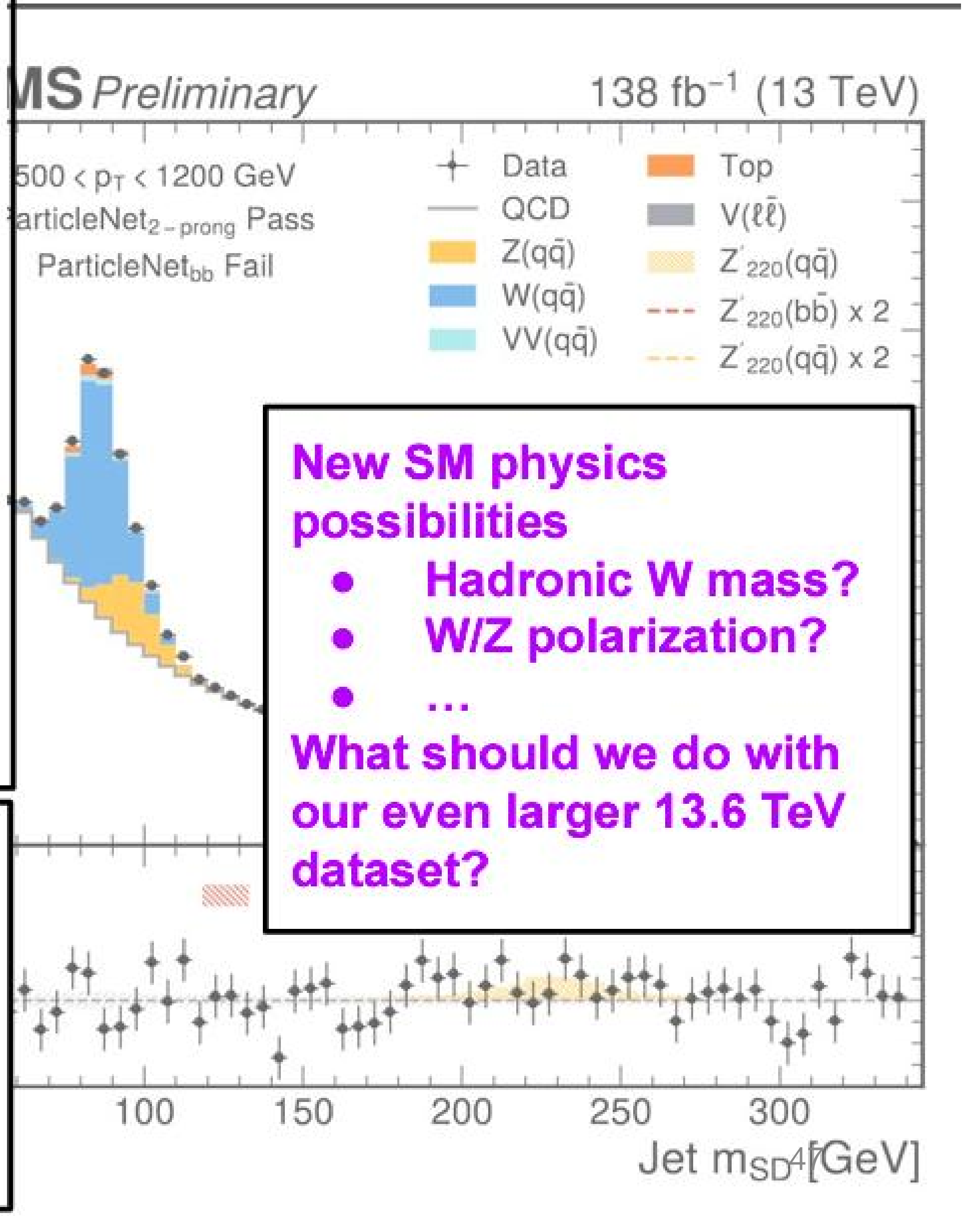

World-leading limits on BSM

- Interpret in terms of vectors, scalars, pseudoscalars
- Limits on g_q scale like lumi^{-4}
- New techniques are driving improvements!

New SM physics possibilities

- Hadronic W mass?
- W/Z polarization?
- ...

What should we do with our even larger 13.6 TeV dataset?

Exotic substructure for exotic Physics: example hadronic LLP: CMS-EXO-23-013

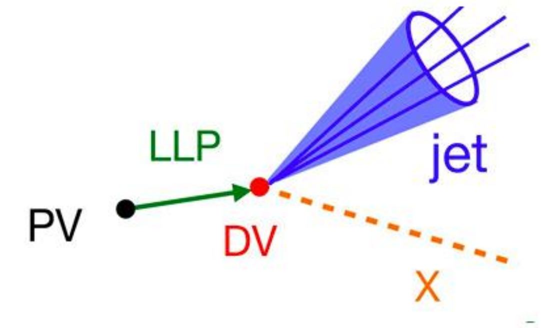

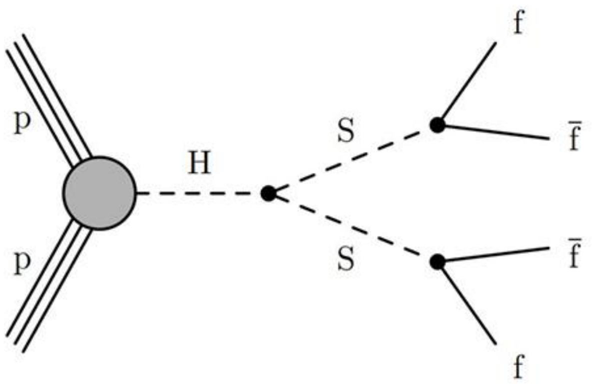

Traditional techniques (trigger and tagging) optimised for prompt jets

Special GNNd developed for displaced vertices

Additional GNNp for prompt production

Background estimated from the comparison of the two using the ABCD method

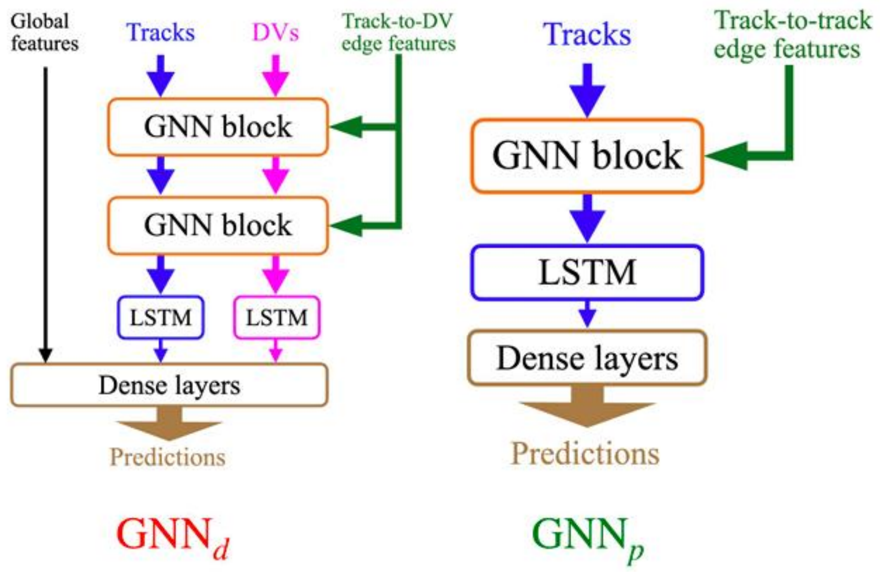

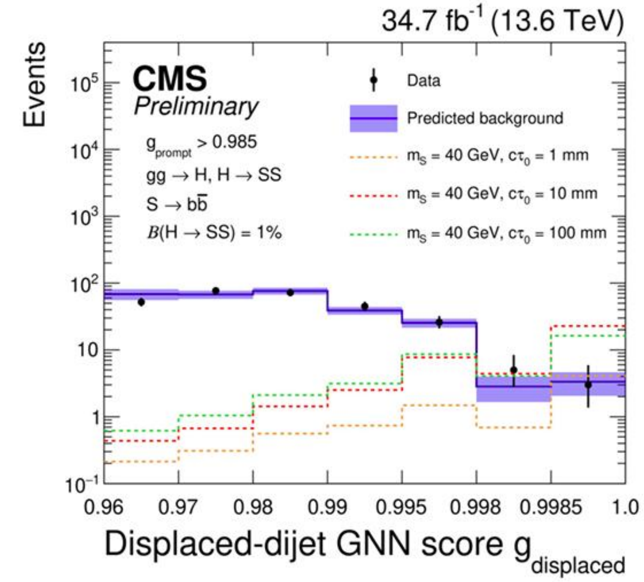

Semi-visible jets

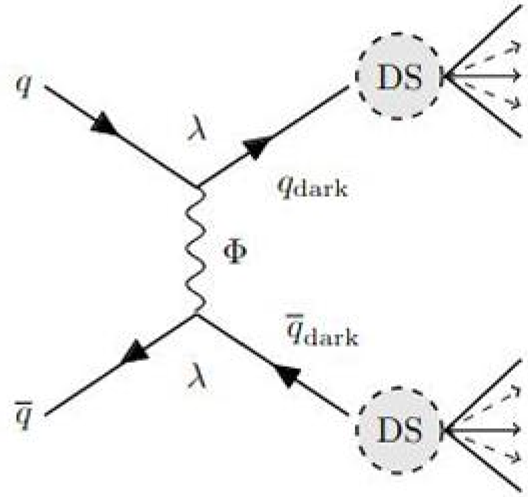

Characterised by ratio of stable partiles in the jet R, that influence Pt balance and ΔΦ

A first fit is performed in low E^T_{miss} CR to get the multijet re-weighting factors.

A final fit of the [pTbalance and Δϕ] 2D distribution, with all high E^T_{miss} regions, is done:

- largest uncs on pTbalance and Δϕ shapes comes from signal, Z+jets and ttbar modelling (10%)

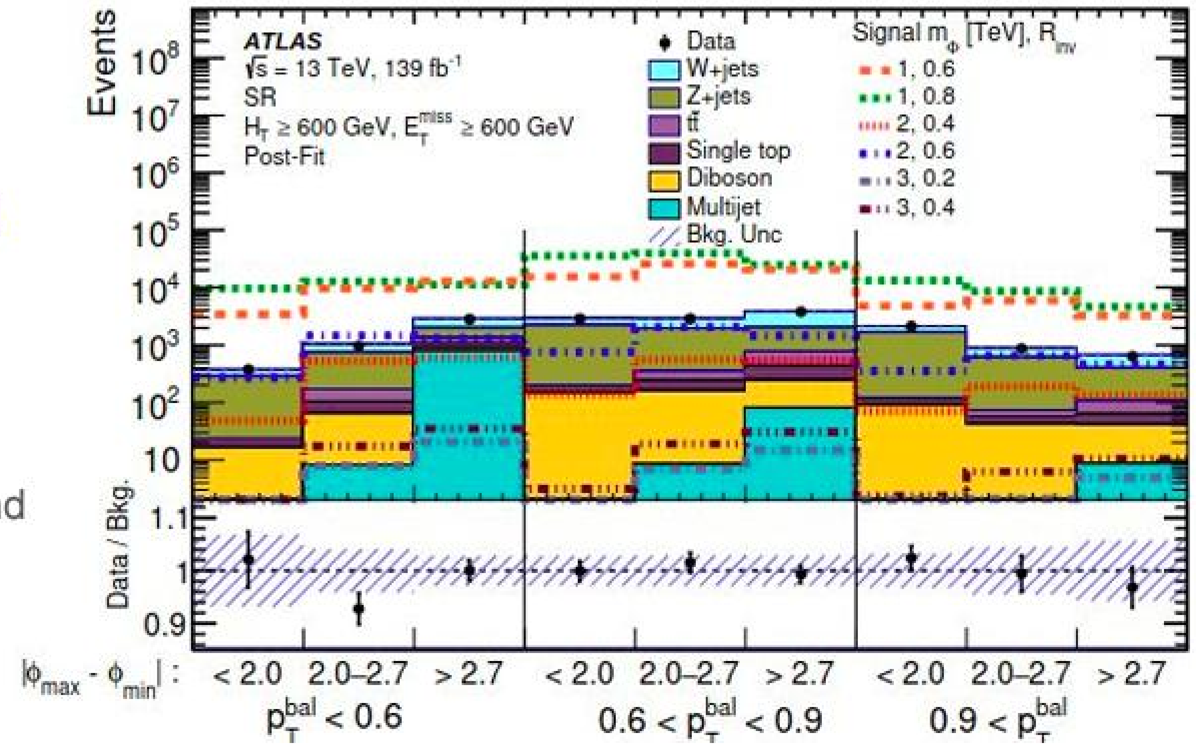

Conclusions

- Jet physics is complex, and extremely important at the LHC
- It has been rapidly evolving, with the development of substructure and Machine Learning
- ML in obiquous, helping us reconstructing and calibrating jet constituents, reducing pileup and calibrating jets
- Sophisticated ML techniques are used for multi-class jet tagging, and exotic searches
- We are only half-way in the LHC explotation, and the next years will see many more jets, boosted objects and pileup
- Even more ingenuity and creativity will be needed